Accepted Manuscript

Mineralogy of low grade metamorphosed manganese sediments of the Urals: Petrological and geological applications

Aleksey I. Brusnitsyn, Elena V. Starikova, Igor G. Zhukov

PII: S0169-1368(16)30397-3
DOI: doi: 10.1016/j.oregeorev.2016.07.004
Reference: OREGEO 1867

To appear in: *Ore Geology Reviews*

Received date: 25 September 2015
Revised date: 5 July 2016
Accepted date: 7 July 2016

MINERALOGY OF LOW GRADE METAMORPHOSED MANGANESE SEDIMENTS OF THE URALS: PETROLOGICAL AND GEOLOGICAL APPLICATIONS

Aleksey I. Brusnitsyn[a*], Elena V. Starikova[b, c], Igor G. Zhukov[d, e]

[a] *Department of Mineralogy, St. Petersburg State University, Universitetskaya Emb. 7/9, St. Petersburg, 199034 Russia*

[b] *JSC «PolarGeo», 24 line, 3–7, St. Petersburg, 199106 Russia*

[c] *Department of Geology of Mineral Deposits, St. Petersburg State University, Universitetskaya Emb. 7/9, St. Petersburg, 199034 Russia*

[d] *Institute of Mineralogy, Urals Branch, Russian Academy of Sciences, Miass, Chelyabinsk District, 456317 Russia*

[e] *National Research South Urals State University, Miass Branch, 8 July str., 10a, Miass, Chelyabinsk District, 456304 Russia*

** Corresponding author. E-mail: brusspb@yandex.ru (A.I. Brusnitsyn)*

ABSTRACT

The paper describes mineralogy of the low grade metamorphosed manganese sediments, which occur in sedimentary complexes of the Pai Khoi Ridge and the Polar Urals and volcanosedimentary complexes of the Central and South Urals. The degree of metamorphism of the rocks studied corresponds to PT conditions of the prehnite–pumpellyite (deposits of Pai Khoi and Polar and South Urals) and green schist (deposits of the Central Urals) facies. One hundred and nine minerals were identified in the manganese-bearing rocks on the basis of optical and electron microscopy, X-ray diffraction, and microprobe analysis. According to the variations in the amount of major minerals of the manganese rocks of the Urals, they are subdivided on carbonate (I), oxide–carbonate–silicate (II), and oxide–silicate (III) types. Carbonates, various Mn^{2+}-bearing silicates associated with oxides and carbonates, and braunite (Mn^{3+}-bearing silicate) are the major Mn hosts in types I, II, and III, respectively. Because of the different oxidation state of Mn, the rocks of types I and II are termed as «reduced» and the rocks of type III, as «oxidized». The formation of a certain mineralogical type of metamorphic assemblage is controlled by the content of organic matter in the primary sediments. The sequence type I → type II → type III reflects the decrease in the amount of organic matter in metalliferous sediments. Mineralogical data indicate that manganese in the primary sediments accumulated in a silicate form (Mn–Si gel, glass, etc). During diagenesis, the Mn–Si phase was transformed to neotokite with subsequent formation of caryopilite and further crystallization of pyroxmangite, rhodonite, tephroite, and other silicates due to reactions involving caryopilite. The hydrated Mn-silicates (caryopilite and/or friedelite) and the spatially associated parsettensite, stilpnomelane, and other minerals are the index minerals of the low grade metamorphism. Under PT conditions of prehnite–pumpellyite facies, nearly 70% of silicate minerals are hydrous. The metamorphosed Mn-bearing sediments are characterized by the low-temperature caryopilite (or tephroite-caryopilite-pyroxmangite ± rhodonite) and the high-temperature caryopilite-free (or tephroite-pyroxmangite ± rhodonite) facies. Their PT conditions correspond to zeolite and prehnite-pumpellyite (the low-temperature) and green schist and higer grade (the high-temperature) facies.

Keywords: Manganese, deposit, caryopilite, genesis, Ural

1. Introduction

Several tens of small stratiform Mn deposits of the Urals are confined to the sedimentary and volcanosedimentary complexes (Betekhtin, 1946; Rabinovitch, 1971; Mikhailov and Rogov, 1985; Mikhailov, 1993, 2001, 2011; Shishkin and Gerasimov, 1995; Magadeev et al., 1997; Ovchinnikov, 1998; Kontar et al., 1999; Kostyuk et al., 2000; Starikova and Zavileisky, 2010; Brusnitsyn and Zhukov, 2005, 2012; Brusnitsyn, 2013*a*; Kuleshov et al., 2014; Starikova, 2014). Most researchers suppose that Mn-bearing ores were formed in marine basins and are syngenetic to host sediments. As known, in the contemporary oceans, Mn is deposited in oxide form and, during diagenesis, catagenesis, and metamorphism, the Mn oxides are transformed into carbonates and silicates. Numerous Mn deposits of the Urals are metamorphosed under conditions of low-grade prehnite-pumpellyite or green schists facies. Under such conditions, Mn rocks are characterized, on the one hand, by the relics of sedimentary protolith and sedimentary-diagenetic textures and structures and, on the other hand, by the presence of typical metamorphic minerals (rhodonite, tephroite, spessartine, and other minerals). The study of these «transitional» rocks provides a unique opportunity to identify the transformation of the phase composition during the gradual increase in temperature and pressure, i.e., during transition of sedimentary rock to metamorphic one.

More than 30 deposits have been studied and the following deposits are chosen for the detailed mineralogical studies (Fig. 1): (i) the deposits, which were metamorphosed under conditions of prehnite-pumpellyite facies: Parnok (Polar Urals) and Kozhaevo, Urazovo, Bikkulovo, Kazgan-Tash, Kusimovo, Kyzyl-Tash and South, Middle, and North Fayzuly (South

Urals); (ii) those, which were metamorphosed under conditions of prehnite-pumpellyite to green schists facies: Kheyakha, Sibirchatayakha, Karsk, Nadeiyakha-1 and -2, Lower Silova, Silovayakha (Pai Khoi) and Sob River basin (Polar Urals); and (iii) the deposits, which were metamorphosed under conditions of green schists facies: Malosedelnikovo, Kurganovo, and Borodulino (Central Urals).

The results of studies of the deposits have previously been published in (Brusnitsyn, 1998, 2000, 2006, 2010, 2013*a*, 2015; Brusnitsyn and Zhukov, 2005, 2012; Starikova and Zavileisky, 2010; Starikova, 2011, 2012, 2014; Brusnitsyn et al., 2000, 2009, 2014, 2016). The aim of this paper is to summarize mineralogy of low-grade metamorphosed Mn-bearing sediments of the Urals and to interpret these data according to the geological and physico-chemical conditions of formation and transformation of metalliferous sediments.

2. Geological background

In the present-day erosion level, the Urals is a longitudinally oriented fold belt with a length of 2500 km and a width from 200 to 450 km. Its geological structure is described in many papers (Zoloev et al., 1981; Puchkov, 2010, 2016; Petrov and Melgunov, 2011). According to the modern concepts, the Urals is an orogenic belt, which was originated on the Precambrian basement in Cambrian–Ordovician, steadily evolving in Ordovician–Devonian, and was deformed during Carboniferrous–Triassic collision. The belt has a zoned structure consisting of a western paleocontinental and an eastern paleooceanic sectors.

The western sector is a fragment of the passive margin of the East European paleocontinent. It includes the Preuralian foredeep composed of the Permian–Triassic molasse, the West Uralian zone of the Paleozoic shelf and bathyal sediments, and the Central Uralian zone, which consists of Precambrian sedimentary, metamorphic, and igneous rocks. The eastern sector represents the fragments of an active paleocontinental margin with complexes of the ocean floor, ensimatic island arcs, and interarc basin, and microcontinent blocks. This sector consists of the Tagil–Magnitogorsk zone with dominant Paleozoic island arc volcanic and volcanosedimentary rocks and the East Uralian and Transuralian zone, which are characterized by intercalation of the uplifted blocks of the Precambrian metamorphic rocks (microcontinents) and the troughs made up of the Silurian–Lower Carboniferous volcanic and sedimentary complexes, the composition of which is similar to those of the Tagil–Magnitogorsk zone. The eastern sector also hosts abundant Late Devonian to Early Carboniferous and Permian granitic intrusions. The western and eastern sectors are bounded by the Main Uralian fault zone, which is the large east-dipping suture with ophiolite massifs and mélange-olistostrome complexes.

The deposits of manganese-bearing rocks are identified along the entire Urals (Kontar et al., 1999; Mikhailov, 2001, 2011). They are confined to various lithotectonic (paleogeodynamic) zones and are located in the rocks of different ages (Fig. 1). The deposits studied in Pai Khoi and Polar Urals occur in sedimentary rocks of passive paleocontiental margin in contrast to the deposits of the South and Central Urals, which are hosted in volcanosedimentary complexes of active paleocontiental margin.

3. Deposits studied

3.1. Deposits in sedimentary rocks

The brief characteristics of the deposits studied are presented in Table 1. The deposits of Pai Khoi and Polar Urals occur in siliceous and clayey-carbonate rocks and black shales of the deep shelf and continental slope.

Pai Khoi. The manganese ores of Pai Khoi were found in the beginning of the 20th century, but were actively studied only in 1970s–1990s and 2006–2014 (Miklyaev, 1991; Yudovich et al., 1998; Yushkin et al., 2007; Starikova and Zavileisky, 2010; Starikova, 2014). The occurrences of manganese ores cover an area more than 80 km long and about 30 km wide. The host rocks are the Upper Devonian carbonate-siliceous, clayey-carbonate-siliceous, and siliceous rocks. A horizon of red jaspers with interlayers of limestones and siliceous shales in the basement of the Mn-bearing stratum is crowned by siliceous shales with variable amounts of carbonate and clayey material. Some shales are enriched in finely dispersed organic matter. The total thickness of the Mn-bearing rocks is 10–30 m. Manganese ores compose the series of beds and flattened lenses 0.2 to 3 m thick and up to several tens to hundreds of meters along the strike. Most of the beds occur in shales, which overlap jaspers; some of them are known inside the jasper horizon.

Polar Urals. Manganese ores of the Polar Urals were studied in the upper reaches of the Sob River basin and in the Parnok deposit.

The ores in the valley of the Sob River basin were found in the 1960s and studied in 1970s–1980s and 2003–2004 (Silayev, 1994; Kostyuk et al., 2000; Brekhunov et al., 2004; Brusnitsyn et al., 2016). Their geological setting is very similar to that of the Pai Khoi deposits. The host rocks are the Upper Devonian to Lower Carboniferous siliceous, carbonaceous-siliceous, and carbonaceous-clayey-siliceous shales. Manganese ores forms the concordant lenses and beds 0.2 to 1.5 m thick and the first tens of meters along the strike. Only small Mn beds were found in this area, however, they occur systematically in the area of 60 km^2 with variable size

The Parnok deposit is one of the largest manganese deposits of the Urals (Shishkin and Gerasimov, 1995; Gerasimov et al., 1999; Zykin, 2004; Brusnitsyn, 2013*b*, 2015; Brusnitsyn et al., 2014). It was discovered in 1987 and has periodically been exploited. The area of the deposit is composed of the terrigenous-carbonate rocks: limestones, siltstones, sandstones, and siliceous and clayey-siliceous-carbonate shales, many of which are carbonaceous. The age of the ore-bearing rocks is a matter of debate: it is either Middle to Late Ordovician (Shishkin and Gerasimov, 1995) or Middle Devonian (Zykin, 2004). The manganese ores are characterized by a complex mineralogy with dominant Mn carbonates and silicates in contrast to extremely homogeneous iron ores, which are composed of magnetite. The alternating beds and layers of Mn and Fe ores occur conformably in black shales and limestones. The thickness of some beds is 2 to 5 m and their length attains 100 m along the strike. The adjacent beds are grouped into the bodies up to 20 m thick and up to 400 m long. The chains of the ore bodies are streched at the distance of up to 4 km.

The sources of manganese in sedimentary rocks could vary (hydrothermal or silt diagenetic fluids, river run-off, etc.). In case of the deposits of Pai Khoi and Polar Urals, the hydrothermal source is the most popular conception (Miklyaev, 1991; Shishkin and Gerasimov, 1995; Yudovich et al., 1998; Brusnitsyn, 2013*b*, 2015; Starikova, 2014). According to this conception, manganese was introduced to the marine basin via hydrothermal fluids, which were circulated in the Paleozoic sediments. The hydrothermal system was most likely triggered by short-term renewed tectono-magmatic processes in the basement of sedimentary complexes. The fluids discharged in seafloor depressions with periodically stagnated conditions. The changes in physico-chemical parameters of seawater were favorable for accumulation of either carbonaceous, ferrous or manganese sediments.

In the Late Paleozoic to Early Mezozoic, the sedimentary strata were intensely deformed and the tectonic processes were accompanied by regional low-grade metamorphism. The metamorphism of rocks of the Parnok deposit corresponds to the conditions of prehnite-pumpellyite facies: T = 200–300 °C and p = 2–2.7 kbar (Gerasimov, 2000; Brusnitsyn, 2015). The degree of metamorphism in the area of the Sob River basin and Pai Khoi was lower than conditions of the green schist facies (Starikova, 2011; Brusnitsyn et al., 2016). All the deposits are characterized by the Mezozoic–Cainozoic oxidation zone, which is mostly composed of Mn oxides and hydroxides.

3.2. *Deposits in volcanic rocks*

By the mode of occurrence and chemical composition, the hydrothermal–sedimentary Mn-bearing rocks of the Central and South Urals are similar to the hydrothermal sediments of active volcanic structures of the present-day oceans (Kheraskov, 1951; Gavrilov, 1972; Kalinin, 1978; Serkov, 1989; Kontar et al., 1999; Brusnitsyn, 2000, 2010; Brusnitsyn et al., 2000, 2009; Mikhailov, 2001; Brusnitsyn and Zhukov, 2005, 2012).

Central Urals. Eleven manganese deposits are known in the area of the city of Yekaterinburg (Serkov, 1989; Goldobin, 1994; Brusnitsyn, 1998, 2000). The most famous Malosedelnikovo deposit was discovered at the end of the 18th century and has been exploited until the 1990s for semiprecious stone (rhodonite), as well as Kurganovo and Borodulino deposits were exploited in the second half of the 20th century. Other deposits were not of economic interest.

The deposits are situated in the East Uralian lithotectonic zone. The Silurian Mn-bearing volcanosedimentary rocks surround the blocks of the Precambrian metamorphic rocks. The Late Paleozoic mafic and felsic intrusives occur in the area of the deposits. The manganese ores are concentrated in siliceous rocks, muscovite-quartz, chlorite-quartz, and carboniferous-quartz schists. The deposits are characterized by the flattened lens-shaped manganese ore bodies, but, more often, the primary lenses are divided into several ellipsoidal or isometric fragments up to 4 m thick and 10 to 30 m long as a result of mechanical deformations (boudinage). The total length of the Mn-bearing rocks is ~500 m. Among the deposits studied, the deposits of the Central Urals are metamorphosed under conditions of green schists facies: T = 450–500 °C and p = 2–3.5 kbar (Serkov, 1989; Brusnitsyn, 2000; Perova, 2004).

South Urals. Eighty four small manganese deposits in the Devonian volcanic rocks of the South Urals are known since the second half of the 20th century (Salikhov et al., 2002). Some of them (Urazovo, Bikkulovo, Kusimovo, Kyzy-Tash, South Fayzuly) were exploited at the beginning of the 20th century, but the works have been terminated to the end of the 1940s. The Kozhaevo, South and North Fayzuly, and Bikkulovo deposits have been mined from 1997 to 2007, but now they are considered uneconomic.

The deposits are confined to the Middle to Upper Devonian volcanosedimentary rocks, which were formed during the final stages of the evolution of the Early to Middle Devonian andesite–basaltic and rhyolite–basaltic complexes. The siliceous rocks (jasperites, jaspers, siliceous siltstones, and tuffites) are widely abundant in the volcanosedimentary complexes. Jasperites are the most striking variety of the siliceous rocks (see Fig. 3a, b in Brusnitsyn and Zhukov, 2012). These are hematite–quartz rocks with globular, colloform, and spherulitic textures and typical brecciated structure. They are currently considered as lithified analogues of

Fe–Si sediments, which are formed on the seafloor close to the low-temperature hydrothermal vents (Kheraskov, 1951; Crerar et al., 1982; Grenne and Slack, 2003; Brusnitsyn, Zhukov, 2012; Zaykov and Ankusheva, 2013; Brusnitsyn, 2013a). In many deposits (Kozhaevo, Urazovo, Kazgan-Tash, Bikkulovo, Kyzyl-Tash, South and Middle Fayzuly), the ore bodies are made up of closely associated manganese ores and jasperites. Such an association is a good evidenceof accumulation of metalliferrous sediments near hydrothermal vents (Brusnitsyn and Zhukov, 2005, 2012; Brusnitsyn, 2013a; Brusnitsyn et al., 2000, 2009). In some deposits (Kusimovo, the northern part of the South Fayzuly, North Fayzuly, Ayusazovo, Gabdimovo), manganese ores occur in jaspers. It is suggested that Mn-bearing sediments accumulated far from the discharge zones of the hydrothermal fluids.

In all cases, manganese ores form conformable lenses and beds in siliceous rocks, volcanomictic sandstones, and tuffites. The thickness of the ore bodies reaches 2.5 m and their length is up to 450 m. By geochemical features (distribution of major, trace and rare earth elements), manganese ores of the South Urals are similar to the present-day hydrothermal sediments (Brusnitsyn et al., 2013). In the Late Devonian to Late Carboniferrous, the volcanosedimentary complexes underwent regional metamorphism of T = 200–250 ºC and p = 2–3 kbar (Necheukhin, 1969; Brusnitsyn and Zhukov, 2012; Brusnitsyn, 2013a). Later, they were deformed during Carboniferous–Permian collision. The Mezozoic–Cainozoic supergene processes are locally manifested at these deposits.

4. Mineral composition of manganese ores

Manganese ores (in addition to the economic definition, the term «ore» in this case also indicates the geochemical composition of Mn-rich rocks) of the Urals are characterized by micro- to fine-grained textures (the mean size of mineral grains is 10–50 μm) and layered, lens-shaped, banded, spotted (brecciated, nodular) or, locally, veinlet structures occur (Fig. 2). One hundred and nine minerals were identified in the manganese rocks on the basis of optical and electron microscopy, X-ray diffraction, and microprobe analysis (Table 2). The manganese rocks are characterized by extremely uneven distribution of minerals, the amount of which strongly varies even within a single ore body. Twenty five to thirty minerals, on average, could be identified in a deposit; six to eight minerals are rock-forming (each mineral composes no less than 5 vol % of rock) and other minerals are subordinate (1–5 %) and accessory (< 1 %). Quartz, tephroite, spessartine, rhodonite, piroxmangite, caryopilite (and/or friedelite), Mn-calcite and rhodochrosite are the most abundant rock-forming minerals. In several deposits, major minerals also include hematite, hausmannite, braunite, Mn-humites (sonolite, alleghaniite, ribbeite), andradite, minerals of the epidote group (Mn-epidote, piemontite), parsettensite, and kutnohorite. Mn-aksinite, minerals of the chlorite group (Mn-clinoxchlore and chamosite, pennantite), and stilpnomelane (locally, K-feldspar, albite, Mn-pyroxenes, amphiboles, and mica) are typical subordinate minerals. The most typical accessory minerals include alabandite, pyrite, pyrophanite, magnetite, neotocite, celsiane, barite, and apatite.

According to the variations in the amount of major minerals in the manganese rocks of the Urals, they are subdivided on carbonate (I), oxide–carbonate-–silicate (II), and oxide–silicate (III) types. Carbonates, various Mn^{2+}-bearing silicates associated with oxides and carbonates, and braunite (Mn^{3+}-bearing silicate) are the major Mn hosts in types I, II, and III, respectively. Because of the different oxidation state of Mn, the rocks of types I and II are termed as «reduced» and the rocks of type III, as «oxidized» (Mottana, 1986; Brusnitsyn, 2007). Each ore type combines several mineralogical ore varieties, which could grade into each other. For example, on the basis of the dominant Mn-mineral, the type I is subdivided into (a) rhodochrosite, (b) siderite-rhodochrosite, and (c) kutnohorite ores. The oxide–carbonate–silicate ores are subdivided into five groups (d–h). Ores of the group (d) mainly consist of hausmannite, rhodochrosite, and tephroite and subordinate pyrochroite, humites, caryopilite, calcite, kutnohorite, and other minerals. The group (e) includes ores, which consist of silicates (tephroite, rhodonite, pyroxmangite, caryopilite and/or friedelite, and minerals of the humite, garnet and epidote groups), quartz, rhodochrosite, and calcite. The ores of the group (f) are similar to those of the group (e), but they contain no caryopillite and/or friedelite. No Mn oxides and tephroite occur in ores of the groups (g) and (h); rhodochrosite is rare. Quartz and rhodonite are dominant in the group (g), whereas quartz and Mn-epidote and/or piemontite are the major minerals in the group (h). The oxide–silicate ores include two groups, which are composed of (i) quartz, hematite and braunite and (j) braunite, rhodonite, piemontite, caryopilite, and calcite.

The mineral composition of manganese ores hosted in sedimentary and volcanosedimentary successions is generally similar. However, no braunite-bearing manganese ores are known in sedimentary rocks. These ores are characterized by the presence of galena, sphalerite, zircon, friedelite, stilpnomelane, K-feldspar, and Ce-minerals (allanite, monacite, Ce-carbonate) in contrast to ores in volcanosedimentary beds with more typical hematite, andradite, grossular, titanite, epidote, piemontite, minerals of the pumpellyite group, Na pyroxenes, and amphiboles. In terms of mineral composition, the manganese ores of the Urals are similar to low-grade metamorphosed Mn-bearing sediments of California, the Alps, Japan, and other regions (Abrecht, 1989; Luccheti, 1991; Flohr and Huebner, 1992; Dasgupta, 1997; Nakagawa et al., 2009, 2011).

5. Discussion

Precipitation of manganese most likely occurred in oxide form of Mn^{3+} and/or Mn^{4+} (amorphous phase, vernadite, todorokite, birnessite) similarly to that in contemporary ocean sediments. Further geological processes transformed significantly the mineral composition of Mn-bearing sediments. The character of diagenetic mineral formation is caused by the content of organic matter in the sediments (Berner, 1980; Brusnitsyn, 2007; Konhauser, 2007; Johnson et al., 2016). Decomposition of organic matter provided anaerobic CO_2-rich reduced conditions favorable for the crystallization of Mn^{2+} carbonates and silicates. If organic matter in primary sediment was minor or absent, Mn preserved the high oxidation state, which prevented from the formation of rhodochrosite.

The deposits of the Urals are characterized by the dominant "reduced" carbonate or oxide–carbonate–silicate manganese ores, the formation of which is related to the biogenic processes. Most Mn carbonates (rhodochrosite, kutnohorite, Mn calcite and siderite) are diagenetic, which is evident from sedimentary diagenetic textures of their aggregates – pelitic, colloform, cloddy, spherulitic, etc. (Fig. 3a–c), which are replaced by coarser-grained mosaic aggregates during the later recrystallization. In Mn-rich ore type (d), isometric and irregular aggregates of hausmannite and pyrochroite are replaced by rhodochrosite, which represent the relics of partly reduced primary sedimentary Mn oxides. The participation of organic matter in the formation of carbonates is supported by carbon isotopic composition. The samples studied are mostly characterized by negative $\delta^{13}C_{carb}$ values (Table 3), which are typical of biogenic carbon (Hoefs, 2009; Polgári et al., 2012, Bodor et al., 2016). The increased carbon isotopic composition is typical only for the kutnohorite ores of Pai Khoi (Kheyakha, Sibirchatayakha and Lower Silova deposits), which were formed, in addition to Mn oxides and organic matter, from sedimentary Ca carbonates enriched with ^{13}C (Starikova and Kuleshov, 2009; Kuleshov et al., 2014). It should be noted that the structures of aggregates of Mn carbonates resemble the products of bacterial activity, e.g., the kutnohorite beds with fine wavy-layered structures are interpreted as stromatolite-like rocks (Starikova, 2012).

During the burial of sediments in the excess of organic matter, the primary sedimentary Mn oxides reacted with opal (and/or quartz), that resulted in the formation of braunite, which crystallized during the early stages of lithogenesis (probably dia- or catagenesis of sediments). This is evident from the well-recognized and well-preserved radiolarians filled with braunite. The braunite-bearing nonmetamorphosed manganese sediments are known, for example, in the deposits of the South Africa (Miyano and Beukes, 1987; Gutzmer and Beukes, 1996; Gutzmer et al., 2002).

The «oxidized», braunite-bearing oxide–silicate ores are rare in the Urals. They are found only in the red siliceous rocks (jaspers), which occur in the Devonian volcanic complexes of the South Urals (Kusimovo, Niyasgulovo-1, Ayusazovo, Gabdimovo, North Fayzuly deposits). Such ores probably mark the deepest marine depressions with low bioproductivity of the water column and supressed benthos. It is interesting that the same stratigraphic level with braunite-bearing ores hosts the manganese ore bodies, which are composed of the «reduced» oxide–carbonate–silicate ores (e.g., South Fayzuly deposit). We believe that these deposits were formed *in situ* of «biological marine oases» around the discharge zones of the low-temperature hydrothermal vents (Zhukov et al., 1998; Zhukov and Leonova, 1999; Brusnitsyn and Zhukov, 2012; Ayupova and Maslennikov, 2013.).

The increase in temperature and pressure results in crystallization of numerous silicates in manganese ores. It is difficult to say now what is the lower temperature level, which is necessary for the mass crystallization of Mn silicates in sediments, however, their overwhelming majority is stable prior to the PT conditions of prehnite-pumpellyite facies.

The diversity and the high contents of hydrous silicates are the typical features of low metamorphic manganese ores. Fifty three silicates are identified in the manganese ores. The H_2O content is 8−12 wt. % in 16 minerals (gageite, greenalite, caryopilite, friedelite, manganpyrosmalite, bementite, kelliite, pennantite, clinochlore, chamosite, stilpnomelane, patsettensite, bannisterite, cumbsite, zussmannite, and neotocite) and is 2−4 wt. % in 22 silicates (minerals of the humite, epidote, pumpellyite, amphibole, and mica groups, ilvaite, heitmanite, manganaxinite, manganbabingtonite, and talc). Thus, about 70 % of metamorphic silicates are hydrated phases.

The Mn–Si minerals with serpentinite-type of crystal structure (caryopilite, friedelite, manganpyrosmalite, bementite) deserve special attention. These minerals are barely distinct from each other, especially when they form complex aggregates. To simplify the description, below we will use only the name caryopilite, which is the most widespread mineral. The genetic relations between serpentine-like minerals are reviewed in detail in Brusnitsyn (2015).

Caryopilite is an index mineral of low-grade metamorphism of manganese sediments; the maximum temperature of its stability corresponds to the upper limit of prehnite-pumpellyite facies (Kato, 1963; Watanabe et al., 1970; Abrecht, 1989; Flohr and Huebner, 1992; Dasgupta, 1997; Nakagawa et al., 2009, 2014; Brusnitsyn, 2010, 2013*a*). Caryopilite is formed from the fine-dispersed and hydrous Mn–Si phase (most likely, X-ray amorphous neotocite, $MnSiO \cdot nH_2O$), which was present in the primary sediment. This is evident from (i) the layer-by-layer distribution of caryopilite, which is parallel to the general layering of sediments (Fig. 2f–d); (ii) the cloddy, globular, cryptocrystalline, and concentrically-zonal textures of its aggregates, which are similar to gel or glass textures (Fig, 3d, c); (iii) the abundant syneresis fractures in caryopilite, which are formed during dehydration (drying) and the decrease in the volume of the fine-dispersed matter; and (iv) the constant presence of isomorphic Mg and Al (typical elements of silicates but not of Mn oxides and carbonates) in composition of caryopilite.

In turn, neotocite, which is the earlier mineral relative to caryopilite, is a typical (locally, rock-forming) constituent of nonmetamorphosed sedimentary and hydrothermal-sedimentary deposits (Alexiev, 1960; Clark et al., 1978; Andruschenko et al., 1985; Smolyaninova, 1992). It is suggested that neotocite is diagenetic and is a result of coagulation of Mn-Si gel in sediments.

Caryopilite is typical of the «reduced» oxide–carbonate–silicate ores in contrast to the «oxidized» braunite ores. As seen from $T-lgf_{O2}$ plot (Fig. 4), the caryopilite–braunite assemblage is stable in the very narrow field, thus, it is rare in nature. For example, in spite of abundant «oxidized» oxide–silicate ores in the South Urals, caryopilite was identified only in rare braunite–rhodonite rocks of the Kusimovo deposit. At the same time, the stability field of caryopilite in the area of the low f_{O2} values is unlimited.

The interrelations between minerals of the oxide–carbonate–silicate ores show that caryopilite is a precursor for the formation of many rock-forming silicates, e.g., crystals of pyroxmangite or rhodonite (in the presence of calcite). The scheme of this process is as follows (reaction 2 in Fig. 5):

$$\underset{\text{caryopilite}}{Mn_5(Si_4O_{10})(OH)_6} + \underset{\text{quartz}}{SiO_2} = \underset{\text{pyroxmangite}}{5\ Mn(SiO_3)} + 3\ H_2O$$

As a result, the quartz–caryopilite assemblage is replaced by caryopilite–pyroxmangite (rhodonite) and pyroxmangite (rhodonite)–quartz assemblages prior to the PT conditions of prehnite-pumpellyite facies (Fig. 3f). This, however, concerns only the most widespread caryopilite with low Fe, Mg, and Al contents. The Al-, Fe-, and Mg-rich caryopilite does not react with quartz, at least, up to 260 ºC that was observed in the rocks of the South Fayzuly deposit in the South Urals (Brusnitsyn, 2006, 2013*a*).

The replacement of caryopilite by tephroite and minerals of the humite group (sonolite, alleganite, ribbeite) is typical (Fig. 3 g, h). Tephroite is most likely a result of interaction between caryopilite and rhodochrosite:

$$\underset{\text{caryopilite}}{Mn_5(Si_4O_{10})(OH)_6} + \underset{\text{rhodochrosite}}{3\ Mn(CO_3)} = \underset{\text{tephroite}}{4\ Mn_2(SiO_4)} + 3\ H_2O + 3\ CO_2$$

Spessartine is formed after reaction of caryopilite with rhodochrosite and clay minerals (Fig. 2c and Fig. 3i). Schematically, this process can be described by the folowing equations:

$$\underset{\text{caryopilite}}{Mn_5(Si_4O_{10})(OH)_6} + 7\ \underset{\text{rhodochrosite}}{MnCO_3} + 4\ \underset{\text{«kaolinite»}}{Al_2(Si_2O_5)(OH)_4} = 4\ \underset{\text{spessartine}}{Mn_3Al_2(Si_3O_{12})} + 7\ CO_2 + 11\ H_2O$$

$$2\ \underset{\text{caryopilite}}{Mn_5(Si_4O_{10})(OH)_6} + \underset{\text{«kaolinite»}}{Al_2(Si_2O_5)(OH)_4} = 4\ \underset{\text{spessartine}}{Mn_3Al_2(Si_3O_{12})} + 7\ \underset{\text{pyroxmangite}}{MnSiO_3} + 8\ H_2O$$

In addition to caryopilite + spessartine + pyroxmangite (rhodonite) ± tephroite (humites) ± rhodochrosite assemblage, the assemblages with pennantite, clinochlore, muscovite, stilpnomelane, patsettensite, and other minerals are formed in the clay aggregates.

The increase in temperature of metamorphism leads to replacement of caryopilite by pyroxmangite (and/or rhodonite) and tephroite (reaction 3 in Fig.5):

$$\underset{\text{caryopilite}}{Mn_5(Si_4O_{10})(OH)_6} = 3\ \underset{\text{pyroxmangite}}{Mn(SiO_3)} + \underset{\text{tephroite}}{Mn_2(SiO_4)} + 3\ H_2O$$

The pyroxmangite (± rhodonite) + tephroite assemblage is typical of the manganese rocks of the Central Urals and sediments from other regions, which underwent metamorphism of green schist facies (Dasgupta, 1997; Brusnitsyn, 2000, 2007).

Summary of our mineralogical observations allows reconstruction of the succession of transformation of the primary gel-like Mn–Si phase in sediments under the increase in temperature and pressure: (i) the formation of diagenetic neotocite, (ii) its replacement by caryopilite; (iii) further crystallization of pyroxmangite, rhodonite, tephroite, and other silicates, and (iv), finally, the formation of the pyroxmangite (± rhodonite) + tephroite assemblage under conditions of green schist facies.

Specifying our results, we should emphasize several important genetic aspects. First, we manage to identify the presence of the fine-dispersed hydrous Mn–Si phase (gel, glass, etc.) in the sediment, whose amount may be rather high. The nature of this protolith and the conditions of its accumulation are still poorly understood. The mineralogical data, however, certainly indicate its possible presence. This was also suggested by previous researchers, in particular, similar ideas on the genesis of caryopilite and orthosilicates (tephroite, alleganite, sonolite) were put forward for the manganese deposits of California (Flohr and Huebner, 1992). The formation of caryopilite during the earliest stages of lithogenesis and its further replacement by rhodonite and/or tephroite was recorded in the deposits of Japan (Watanabe et al., 1970; El Rhazi and Hayashi, 2003; Nakagawa et al., 2009).

Second, it is evident that, at low temperatures, many manganese silicates are formed at the expense of consecutive transformations precisely of the Mn–Si phase. These processes should be more energetically favorable relative to the crystallization of silicates via reactions of

SiO_2 with Mn oxides and/or carbonates. Thus, Mn silicates crystallize during low grade metamorphism or even pre-metamorphic stages of lithogenesis.

Third, the identification of the low-temperature caryopilite (or tephroite–caryopilite–pyroxmangite ± rhodonite) and high-temperature caryopilite-free (or tephroite- pyroxmangite ± rhodonite) facies is reasonable in the metamorphosed manganese sediments. The PT conditions of the first and second facies correspond approximately to the conditions of the zeolite and prehnite-pumpellyite and green schist and more intense facies, respectively.

Three key consecutive reactions under the gradual increase in temperature, which discriminate the most important stages of lithogenesis, are shown in the T–X_{CO2} plot (Fig. 3a): (reaction 1) the decomposition of neotocite with formation of quartz and caryopilite corresponds to the upper temperature limit of diagenesis; (reaction 2) the reaction of caryopilite with quartz and formation of pyroxmangite (all metamorphic minerals exist in the rock above this reaction); and (reaction 3) the decomposition of caryopilite with formation of tephroite and pyroxmangite, which corresponds to the transition from assemblages of weakly metamorphosed rocks to those of intensely metamorphosed rocks. It is also seen that the assemblages of hausmannite and silicates are stable at the low CO_2 content in the pore fluid. As X_{CO2} increases, hausmannite is replaced by rhodochrosite and the silicate + rhodochrosite assemblage becomes stable. Finally, the highest X_{CO2} values are favorable for crystallization of the rhodochrosite + quartz assemblage, which is typical of many manganese deposits. The rhodochrosite + quartz assemblage is stable in the wide temperature range and pyroxmangite is formed at the expense of this assemblage (reaction 4) at the higher temperatures relative to the reactions with caryopilite. Similarly, tephroite is formed at the expense of reaction of pyroxmangite + rhodochrosite (reaction 5) also at temperatures higher than reactions involving caryopilite. The calculations of reactions (4) and (5) (Fig. 3b) showed that, at T <250°C, silicates could form only at the lowest CO_2 content in pore fluid: for p = 2 kbar, X_{CO2} is < 0.00025 (lgf_{CO2} < –0.13) and the increase in pressure up to 3 kbar decreases the required X_{CO2} value almost in two times.

Thus, a combination of the following factors is necessary for the formation of Mn silicates at low temperatures: (i) the accumulation of manganese in sediments in the form of Mn–Si phase (gel, neotokite); (ii) the presence of organic matter for the reduced conditions; and (iii) the moderate content of organic matter to produce the low CO_2 content. Otherwise, the rhodochrosite + quartz assemblage will be stable instead of silicates.

The major problem concerns the genesis of the primary Mn–Si phase. It is most likely formed as a result of mixing of the hydrothermal fluids with cold seawater. The abrupt change in the physico-chemical conditions brings about the fast loss of elements dissolved in hydrothermal fluids. Manganese and Si are concentrated not only in amorphous or poorly crystallized oxides, but also in the form of metastable Mn-Si phase. If Mn and Si are deposited under the calmer conditions (at significant distance from hydrothermal vents or without hydrothermal fluids), the formation of the Mn–Si phase is unlikely.

Thus, the presence of the low-temperature Mn silicates indicates the hydrothermal genesis of Mn-bearing sediments that is supported by the study of the deposits of the Urals and, especially, South Urals. As was noted above, two types of Mn-bearing rocks are distinguished: those, which were formed within the discharge zone of the hydrothermal fluids, and those, which were formed at the distance from hydrothermal vents (Brusnitsyn and Zhukov, 2012; Brusnitsyn, 2013*a*). Diverse Mn silicates are identified only in the deposits of type (1) (Urazovo, Kozhaevo, Bikkulovo, Kazgan-Tash, Kyzyl-Tash, South and Middle Fayzuly). The Mn ore bodies of type (2) (North Fayzuly, the northern part of the South Fayzuly, Kusimovo) are made up of monotonous quartz–braunite ores (Table 1). The hydrothermal genesis of oxide–carbonate–silicate ores of the deposits of Pai Khoi and Polar Urals is not so obvious. The geological structure of the ore bodies, their mineralogical similarity with ores from the South Urals, and similar metamorphic conditions, however, allow us to suggest their deposition in the discharge zone of hydrothermal fluids.

In addition to the presence of caryopilite and associated hydrated silicates, the low-grade metamorphism of manganese deposits is evident from the following features:

(i) The presence of pyroxmangite $MnMn_6(Si_7O_{21})$. According to experimental data (Maresch and Mottana, 1976), it is stable at p = 2 kbar and T < 420 °C and at p = 4 and T < 450 °C. Its polymorphic analogue Ca-free rhodonite $MnMn_4(Si_5O_{15})$ should crystallize under the same pressures and higher temperatures. The Ca-bearing rhodonite $CaMn_4(Si_5O_{15})$ crystallizes under significantly lower temperatures and pressures, that is established in the deposits studied;

(ii) The presence of johannsenite $CaMn(Si_2O_6)$. The experimental data (Angel, 1984) showed that it is stable at p = 2 and 3 kbar and T <320 and <350°C, respectively. Its polymorphic analogue bustamite $Ca_3Mn_3(Si_3O_9)_2$ would crystallize under the same pressures but the higher temperatures;

(iii) The presence of the minerals of the pumpellyite group, especially Fe and Mn varieties (Schiffman and Liou, 1983; Liou et al., 1985; Bokiya, 1996);

(iv) Mainly fine-grained ores with relics of typical sedimentary-diagenetic structures and textures and micro- and macrofauna; defect (microblocky, poikilitic, etc.) crystal morphology of many minerals (Fig. 3); well-formed grains and mosaic, grano- and heteroblastic, and other metamorphic textures typical of the rocks beginning from green schist facies.

6. Conclusions

The low-grade metamorphosed manganese sediments of the Urals are composed of three ore types: (I) carbonate, (II) oxide–carbonate–silicate, and (III) oxide–silicate. Carbonates, various Mn^{2+}-bearing silicates associated with oxides and carbonates, and braunite (Mn^{3+}-bearing silicate) are the major Mn hosts in types I, II, and III, respectively. Because of the different oxidation state of Mn, the rocks of types I and II are termed as «reduced» and the rocks of type III, as «oxidized». The formation of a certain mineralogical type of metamorphic assemblages is controlled by the content of organic matter in the primary sediments. The consequence type I → type II → type III reflects the decrease in the amount of organic matter in metalliferous sediments. Mineralogical data show that Mn in the primary sediments could accumulate in both oxide and silicate forms (Mn–Si gel, glass, etc). As PT parameters increased, the Mn–Si phase was diagenetically transformed to neotocite, which was further replaced by caryopilite and pyroxmangite, rhodonite, tephroite and other silicates at the expense of reactions with caryopilite. The recognition of the low-temperature caryopilite (or tephroite–caryopilite–pyroxmangite ± rhodonite) and high-temperature caryopilite-free (or tephroite–pyroxmangite ± rhodonite) facies is reasonable in the metamorphosed manganese sediments. The pT-conditions of the first and second facies correspond approximately to those of zeolite and prehnite-pumpellyite and green schist and more intense facies, respectively.

Acknowledgements

This work was supported by the Russian Foundation for Basic Research (project no. 12-05-00308a) and conducted using the analytical opportunities of the «X-Ray Diffraction Methods of Research», «Microscopy and Microanalysis» and «Geomodel» Resource Centers of St. Petersburg State University. This work was supported by the Russian Foundation for Basic Research (project nos 12-05-00308, 16-05-0027) and State Contract AAAA-A16-116021010244-0.

The authors thank Professor Franco Pirajno, Professor Márta Polgári, Professor Masahara Nakagawa, Professor Anatoly Zaytsev, Olga Plotinskaya, Irina Melekestseva and the Editorial Board for the useful suggestions. Igor G. Zhukov thanks Professor Daizo Ishiyama, administration and staff of the Center for Geo-Environmental Science (CGES), Graduate School of Engineering and Resource Science, Akita University (Akita, Japan) for help in analytical works.

References

Abrecht, J., 1989. Manganiferous phyllosilicate assembages: occurrence, compositions and phase relations in metamorphosrd Mn deposits. Contrib. Mineral. Petrol. 103, 228−241.

Alexiev, B., 1960. Neotocite of Oligocene manganese ore horizon of Varnenski region. Mineralogical collection of Lviv Geol. Society 14, 208−214. (in Russian).

Andruschenko, P.F, Suslov, A.T., Gavashvili, N.V., 1985. Manganese ore deposits of Tetrittskaroi ore region of Georgia (USSR). Volcanosedimentary and hydrothermal deposits of manganese (Central Kazakhstan, Lesser Caucasus, Yenisei Ridge). Nauka, Moscow, pp. 115−172. (in Russian).

Angel, R. J., 1984. The experimental determination of the johannsenite/bustamite equilibrium inversion boundary. Contrib. Mineral. Petrol. 85, 272–278.

Ayupova, N.R., Maslennikov, V.V., 2013. Biomorphic textures in the ferruginous–siliceous rocks of massive sulfide bearing paleohydrothermal fields in the Urals. Lithol. Miner. Resour. 48. 438–455.

Berner R.A., 1980. Early diagenesis – a theoretical approach. Princton: Princton Univ. Press., 241 pp.

Betekhtin, A.G., 1946. Economic manganese ores of the USSR. AN USSR, Moscow, 315 pp. (in Russian).

Bodor, S., Polgári, M., Szentpétery, I., Földessy, J. 2016. Microbially mediated iron ore formation, Silicic Superunit, Rudabánya, Hungary. Ore Geol. Rev. 72, 379–401.

Bokiya, G.B., (Eds.) Minerals. Directory., 1996. Nauka, Moscow. Vol. IV. Issue 3. 426 pp. (in Russian).

Brekhunov, A.M., Ostrovsky, L.Y, Pokazanev, V.N. Ilyushenkov, A.Ya., 2004. Mn-bearing potential of volcanosedimentary complexes of the Polar Urals. In: Proceedings of the 2nd Polar Urals Scientific Practical Conference The Polar Urals – the development strategy. Tyumen–Salekhard, pp. 57–67. (in Russian).

Brusnitsyn, A.I. Kuleshov, V.N., Perova, E.N., Zaitsev, A.N., 2016. Carbonate ferromanganese metasediments of the Sob River basin, the Polar Urals: geological setting, composition, genesis. Lithol. Miner. Resour. (in press).

Brusnitsyn, A.I., 1998. Mineralogy of rhodonite deposits of the Central Urals. Zapiski RMO (Proceedings of the Russian Mineralogical Society). 3. 1–11. (in Russian).

Brusnitsyn, A.I., 2000. Rhodonite deposits of the Central Urals (mineralogy and genesis). St. Petersburg State University, St. Petersburg. 200 pp. (in Russian).

Brusnitsyn, A.I., 2006. Mineralogy and conditions metamorphism of manganese ore at the South Faizulino deposit, the Southern Urals, Russia. Geol. Ore Deposits, 2006. 48 (3). 225–248.

Brusnitsyn, A.I., 2007. Associations of Mn-bearing minerals as indicator of oxygen fugacity during the metamorphism of metalliferous deposits. Geochemistry International 45. 345–363.

Brusnitsyn, A.I., 2010. Mineralogy of Metamorphosed Manganese Deposits of the South Urals. Geol. Ore Deposits, 52 (7). 551–565.

Brusnitsyn, A.I., 2013a. Mineralogy of Mn-bearing metasediments of the South Urals. St. Petersburg State University & OJSC «IPK KOSTA», St. Petersburg, 160 pp. (in Russian).

Brusnitsyn, A.I., 2013b. Geochemistry and Genetic Model of the Ore-Bearing Sediments of the Parnok Ferromanganese Deposit, Polar Urals. Geochemistry International 51 (8), 623–645.

Brusnitsyn, A.I., 2015. Parnok ferromanganese deposit (Polar Urals, Russia): mineralogy, geochemistry and genesis of ores. Institute of Earth Sciences, St. Petersburg, 116 pp. (in Russian).

Brusnitsyn, A.I., Kuleshov, V.N., Kalugin, P.S., 2014. Genesis of Carbonates from the Parnok Ferromanganese Deposit, Polar Urals. Lithol. Miner. Resour., 49 (4). 320–335.

Brusnitsyn, A.I., Letnikova, E.F., Zhukov, I.G., 2013. Geochemistry of rare earth and trace elements in Mn-bearing metasediments of the South Urals. In: Sedimentary basins, sedimentation and postsedimentation processes in geological history. IPGG SB RAS, Novosibirsk, 1. 18–121. (in Russian).

Brusnitsyn, A.I., Starikova, E.V., Zhukov, I.G., 2000. The Kyzyl-Tash manganese deposit (Southern Urals, Russia): the Devonian prototype of a lower-temperature hydrothermal mounds of the modern ocean. Geol. Ore Deposits 42 (3), 205–220.

Brusnitsyn, A.I., Zhukov, I.G., 2005. The South Faizuly manganese deposit in the Southern Urals: geology, petrography, and formation conditions. Lithol. Miner. Resour. 40 (1), 30–47.

Brusnitsyn, A.I., Zhukov, I.G., 2012. Manganese deposits of the Devonian Magnitogorsk Pakeovolcanic belt (Southern Urals, Russia). Ore Geol. Rev. 47. 42–58.

Brusnitsyn, A.I., Zhukov, I.G., Kuleshov, V.N., 2009. The Bikkulovskoe manganese deposit (South Urals): geological setting, composition of metalliferous rocks and formation model. Lithol. Miner. Resour. 44 (6), 557–578.

Clark, A. M., Easton, A. J., Jones, G. C., 1978. A study of the neotocite group. Miner. Mag. 42. M26−M30.

Crerar, D. A., Namson, J., Chyi, M. S., Williams, L., Feigenson, M. D., 1982. Manganiferous cherts of the Franciscan assemblage. I. General geology, ancient and modern analogues, and implications for hydrothermal convection at oceanic spreading centers. Econ. Geol. 77 (3). 519−540.

Dasgupta, S., 1997. P–T–X relationships during metamorphism of manganese-rich sediments: current status and future studies. Manganese mineralization: geochemistry and mineralogy of terrestrial and marine deposits. Geol. Soc. Special publication. London, 19. 327–337.

El Rhazi, M., Hayashi, K.I., 2003. Origin and formational environment of Noda-Tamagawa manganese ore, northeast Japan: constraints from isotopic studies. Chem. Erde. 63. 149–162.

Flohr, M. J. K., Huebner, J. S., 1992. Mineralogy and geochemistry of two metamorphosed sedimentary manganese deposits, Sierra-Nevada, California, USA. Lithos. 29. 57−85.

Gavrilov, A.A., 1972. Exhalative-sedimentary mineralization of the Urals and Kazakhstan. Nedra, Moscow. 215 pp. (in Russian).

Gerasimov, N.N., 2000. Geological structure and genesis of the Parnok ferromanganese deposit (Polar Urals). [Doctor dissertation]. Moscow: Moscow State University; 24 pp. (in Russian).

Gerasimov, N.N., Nasedkina, V.Kh., Onishchenko, S.A., Shishkin, M.A., 1999. Mineral composition of ores of the Parnok ferromanganese deposit (Polar Urals, Russia). Geol. Ore Deposits, 1. 84–96.

Goldobin, A.B., 1994. Rhodonite. Mining Journal. Ural Mining Review. 11–12. 20–29. (in Russian).

Grenne, T., Slack, J. F., 2003. Bedded jaspers of the ordovican Lokken ophiolitr, Norway: seafloor deposition and diagenetic maturation of hydrothermal plume-derived silica-iron gels. Miner. Deposita 38. 625–639.

Gutzmer, J., Beukes, N. J., 1996. Mineral paragenesis of the Kalahari manganese field, South Africa. Ore Geol. Rev. 11. 405–428.

Gutzmer, J., Schaefer, M. O., Beukes, N. J., 2002. Red bed-hosted oncolitic manganese ore of the paleoproterozoic Soutpansberg group, Bronkhorstfontein, South Africa. Econ. Geol. 97. 1151–1166.

Hoefs, J., 2009. Stable isotope geochemistry. Berlin Heidelberg: Springer-Verlag. 285 pp.

Johnson, J.E., Webb, S.M., Ma, C., Fischer, W., 2016. Manganese mineralogy and diagenesis in the sedimentary rock record. Geochim. Cosmochim. Acta. 173. 210–231.

Kalinin, V.V., 1978. Manganese and ferromanganese deposits of the eastern slope of the South Urals. In: Manganese Deposits of Foldbelts in the USSR. Nauka, Moscow, pp. 55–90. (in Russian).

Kato, T., 1963. New data on the so-called bementite. Journal Japan Assoc. Miner. Petrol. Econ. Geol. 49. 93−103.

Kheraskov, N.P., 1951. Geology and genesis of manganese deposits of the Eastern Bashkiria. In: Problems of lithology and stratigraphy of the USSR. In the memory of Academician A.D. Arkhangelskiy. Academiyan Nauk SSSR, Moscow, pp. 47–65. (in Russian).

Konhauser, K., 2007. Introduction to geomicrobiology. New York; London: Blackwell Publishing. 425 pp.

Kontar, E.S., Savel'eva, K.P., Surganov, A.V., Aleshin, B.M., Shishkin, M.A., Gerasimov, N.N., Kostromin, D.A., Papulova, O.B., Sergeeva, V.V., 1999. Manganese deposits of the Urals. Ural. Geologos'emochnaya Ekspeditsiya, Yekaterinburg. 120 pp. (in Russian).

Kostyuk, B.F, Ostrovsky, L.Y, Penchuk, V.N Ilyushenkov, A.Y., 2000. Mn-bearing potential of the Polar Urals. The state of manganese ore base in Russia and problems of manganese industry ensuring. Proceedings of I Scientific-Technical Conference. JSC "Ural Institute of Metals", Yekaterinburg, pp. 74–91. (in Russian).

Kuleshov, V.N., Brusnitsyn, A.I., 2005. Isotopic composition ($\delta^{13}O$, $\delta^{18}O$) and origin of carbonates from manganese deposits of the South Urals. Lithol. Miner. Resour. 40, 364–375.

Kuleshov, V.N., Brusnitsyn, A.I., Starikova, E.V., 2014. Manganese Deposits in Northeastern European Russia and the Urals: Isotope Geochemistry, Genesis, and Evolution of Ore Formation. Geol. Ore Deposits 56 (5), 380–394.

Liou, J. G., Maruyama, S., Cho M., 1985. Phase equilibria and mineral parageneses of metabasites in low-grade metamorphism. Miner. Mag. 49. 321−333.

Lucchetti, G., 1991. Tephroite from Val Graveglia metacherts (Liguria, Italy): mineral data and reaction for Mn-silicates and Mn−Ca-carbonates. Eur. J. Miner. 3. 63−68.

Magadeev, B.D., Greshilov, A.I., Radchenko, B.B., 1997. Ore and non-metalliferrous deposits of the Republic of Bashkortostan. Otechestvennaya Geologiya (National Geology). 7. 5−12. (in Russian).

Maresch, W.V., Mottana, A., 1976. The pyroxmangite-rhodonite transformation for the $MnSiO_3$ composition. Contrib. Miner. Petrol. 55. 69−79.

Mikhaylov, B.M., 1993. Manganese ores of Russia. Lithol. Miner. Resour. 4. 23−33.

Mikhaylov, B.M., 2001. Topical problems of prediction of manganese deposits in the Urals. Lithol. Miner. Resour. 1 (36). 1–12.

Mikhaylov, B.M., 2011. Manganese. Geology and Mineral Resources of Russia. In: West of Russia and the Urals. Vol. 1. Book 2. Urals. VSEGEI, St. Peterburg, pp. 319–332. (in Russian).

Mikhaylov, B.M., Rogov, V.S., 1985. Geological prerequisites for manganese deposits forecast in the Urals. Sovet. Geol. 8. 24–31. (in Russian).

Miklyayev, A.S., 1991. Upper Devonian sediments of the Pai Khoi schist zone and their ore-bearing potential. In: The Geology of Devonian sediments of the European North-East part of the USSR. IG KSC UB RAS, Syktyvkar, pp. 52–53. (in Russian).

Miyano, T., Beukes, N. J., 1987. Physicochemical environments for the formation of quartz-free manganese oxide ores from the early proterozoic Hotazel formation, Kalahari manganese field, South Africa. Econ. Geol. 82. 706−718.

Mottana, A., 1986. Blueschist-facies metamorphism of manganiferous cherts: a review of the alpine occurrences. In: Evans, B.W., Brown, H. (Eds.), Blueschist and Eclogites. Geological Society America Mineralogy, pp. 267–299

Nakagawa, M., Fukuoka, M., Kakehi, K., Kakiuchi, G., Tamaki, Y., Taniguchi, T., 2014. Caryopilite and greenalite from the manganese deposits in Shikoku, Southwest Japan. Clay Science 18, 79–86.

Nakagawa, M., Santosh, M., Maruyama, S., 2009. Distribution and minerals assemblages of bedded manganese deposits in Shikoku, Southwest Japan: implications for accretion tectonics. Gandwana Research. 16. 609–621.

Nakagawa, M., Santosh, M., Maruyama, S., 2011. Manganese formations in the accretionary belts of Japan: implications for subduction–accretion process in active convefgent margin. Jour. Asian Earth Scien. 42. 208–222.

Necheukhin, V.M., 1969. Regional greenstone metamorphism of volcanic rocks of the Baymak region of the South Urals. In: Metamorphism of rocks in the Main Volcanogenic Zone of the Urals. Nauka, Moscow, pp. 5–119. (in Russian).

Ovchinnikov, L.N., 1998. Mineral resources and metallogeny of the Urals. Geoinformatik, Moscow. 413 pp. (in Russian).

Perova, E.N., 2004. Physico-chemical model of formation of the metamorphosed silicate manganese deposits. St. Petersburg State University, St. Petersburg. 210 pp. (in Russian).

Petrov, B.V., Melgunov, A.N. (Eds.) 2011. Geology and Mineral Resources of Russia. West of Russia and the Urals. Vol. 1. Book 2. Ural. VSEGEI, St. Peterburg. 583 pp. (in Russian).

Polgári, M., Hein, J.R., Vigh, T., Szabó-Drubina, M., Fórizs, I., Bíró, L., Müller, A., Tóth, A.L. 2012. Microbial processes and the origin of the Úrkút manganese deposit, Hungary. Ore Geol. Rev. 47, 87–109.

Puchkov, V.N., 2010. Geology of the Urals and Cis-Urals (topical problems of stratigraphy, tectonics, geodynamics and metallogeny). DesignPoligraphService, Ufa. 280 pp. (in Russian).

Puchkov, V.N., 2016. General features relating to the occurrence of mineral deposits in the Urals: What, where, when and why. Ore Geol. Rev. (this issue).

Rabinovich, S.A., 1971. The Northern-Urals manganese basin. Nedra, Moscow. 264 pp. (in Russian).

Salikhov, D.N., Kovalev, S.G., Brusnitsyn, A.I., Belikova, G.I., Berdnikov, P.G., Semkova, T.A., Sergeeva, E.V., 2002. Mineral Resources of the Republic of Bashkortostan: Manganese Ores. Institute of Geology, Ufa. 243 pp. (in Russian).

Schiffman, P., Liou, J. G., 1983. Synthesis of Fe-pumpellyite and its stability relations with epidote. J. of Metamorphic Geology 1. 91−101.

Serkov, A.N. 1989. Petrology, mineralogy and genesis of rhodonite deposits of the Central Urals. [Doctor dissertation]. Sverdlovsk. 19 pp. (in Russian).

Shishkin, M.A. Gerasimov, N.N., 1995. The Parnok ferromanganese deposit (Polar Urals). Geol.Ore Deposits 5. 442–452.

Silaev, V.I., 1994. Geochemistry and mineralogy of manganese carbonates of the Polar Urals. In: Lithogenesis and geochemistry of sedimentary formations of the Timan-Urals region. IG KSC UB RAS, Syktyvkar. pp. 60–70. (in Russian).

Smolyaninova, N.N., (Eds.) Minerals. Directory., 1992. Nauka, Moscow. Vol. IV. Issue 1. 630 pp. (in Russian).

Starikova, E.V., 2011. Mineralogy of rhodonite-bearing rocks of the Silovayakhinskoye occurrence, Pai Khoi. Zapiski RMO (Proceedings of the Russian Mineralogical Society) 5. 75–91. (in Russian).

Starikova, E.V., 2012. Stromatolite-like manganese rocks of Pai Khoi. Vestnik St. Petersburg University. Ser. 7. Issue 1. 10–21. (in Russian).

Starikova, E.V., 2014. Famenian manganese-bearing formation of Pai Khoi. Litosfera (Lithosphere) 1. 58–80. (in Russian).

Starikova, E.V., Kuleshov, V.N., 2009. Mechanism of formation of kutnahorite from the Famennian Mn-bearing rocks of Pai Khoi: mineralogical and isotopic data. In: Metallogeny of Ancient and Modern Oceans – 09. Models of ore formation and estimation of deposits. IMin UB RAS, Miass, pp. 234–239. (in Russian).

Starikova, E.V., Zavileisky, D.I., 2010. Geological Setting and Mineral Composition of Famennian Manganese Ores in the Lemva Zone of Pai Khoi: Evidence from Ore Occurrences of the Nizhny Silov Group. Lithol. Miner. Resour. 45. 341–357.

Watanabe, T., Yui, S., Kato, A., 1970. Bedded manganese deposits in Japan, a review. Volcanism and Ore Genesis (Tatsumi T. (ed.)). University of Tokyo Press, pp. 119–142.

Yudovich, Y.E., Belyaev, A.A., Ketris, M.P., 1998. Geochemistry and ore genesis of black shales of Pai Khoi. Nauka, St. Petersburg. 366 pp. (in Russian).

Yushkin, N.P., Kunz, A.F., Timonin, N.I., 2007. Minerageny of Pai Khoi. UB RAS, Yekaterinburg: 291 pp. (in Russian).

Zaykov, V.V., Ankusheva, N.N., 2013. Hematite-quartz mounds of the Lis'y Gory Au-bearing field: a result of hydrothermal activity in the Magnitogorsk paleoisland arc zone. Litosfera (Lithosphere) 5. 57–74. (in Russian).

Zhukov, I.G., Leonova, L.V., 1999. Benthic fauna from hydrothermal edifice of the Fayzuly low-temperature hydrothermal field (South Urals). In: Metallogeny of Ancient and Modern Oceans – 99. Ore Potential of Hydrothermal Systems, IMin UB RAS, Miass, pp. 74–79. (in Russian).

Zhukov, I.G., Mizens, L.I., Sapel'nikov, V.P., 1998. The finding of benthic fauna in the low-temperature paleohydrothermal field of the South Fayzuly manganese deposit (South Urals). In: Metallogeny of Ancient and Modern Oceans – '98: Ores and Genesis of Deposits. IMin UB RAS, Miass, pp. 111–115. (in Russian).

Zoloev, K.K., Rapoport. M.C. Popov. B.A. et al., 1981. The geological evolution and metallogeny of the Urals. Nedra, Moscow. 256 pp. (in Russian).

Zykin. N.N., 2004. Geological structure and genesis of the Parnok ferromanganese deposit (Polar Urals). Vestnik MGU. Ser. Geol. 2. 40–49. (in Russian).

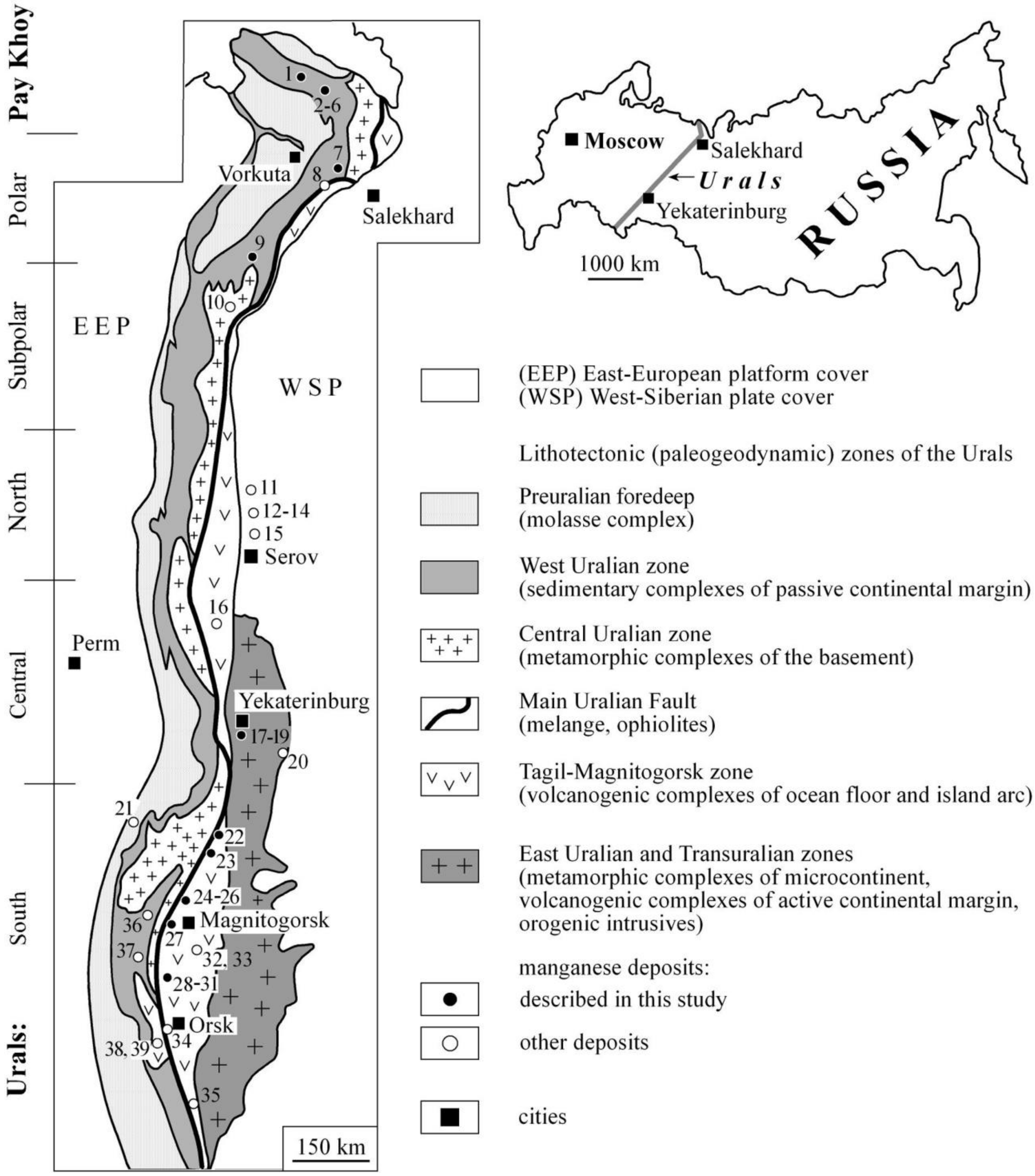
Urals:
Pay Khoy
Polar
Subpolar
North
Central
South
EEP
WSP
Vorkuta
Salekhard
Serov
Perm
Yekaterinburg
Magnitogorsk
Orsk
1
2-6
7
8
9
10
11
12-14
15
16
17-19
20
21
22
23
24-26
27
28-31
32, 33
34
35
36
37
38, 39
150 km
Moscow
Salekhard
Urals
Yekaterinburg
RUSSIA
1000 km
(EEP) East-European platform cover
(WSP) West-Siberian plate cover
Lithotectonic (paleogeodynamic) zones of the Urals
Preuralian foredeep
(molasse complex)
West Uralian zone
(sedimentary complexes of passive continental margin)
Central Uralian zone
(metamorphic complexes of the basement)
Main Uralian Fault
(melange, ophiolites)
Tagil-Magnitogorsk zone
(volcanogenic complexes of ocean floor and island arc)
East Uralian and Transuralian zones
(metamorphic complexes of microcontinent,
volcanogenic complexes of active continental margin,
orogenic intrusives)
manganese deposits:
described in this study
other deposits
cities

Figure 1

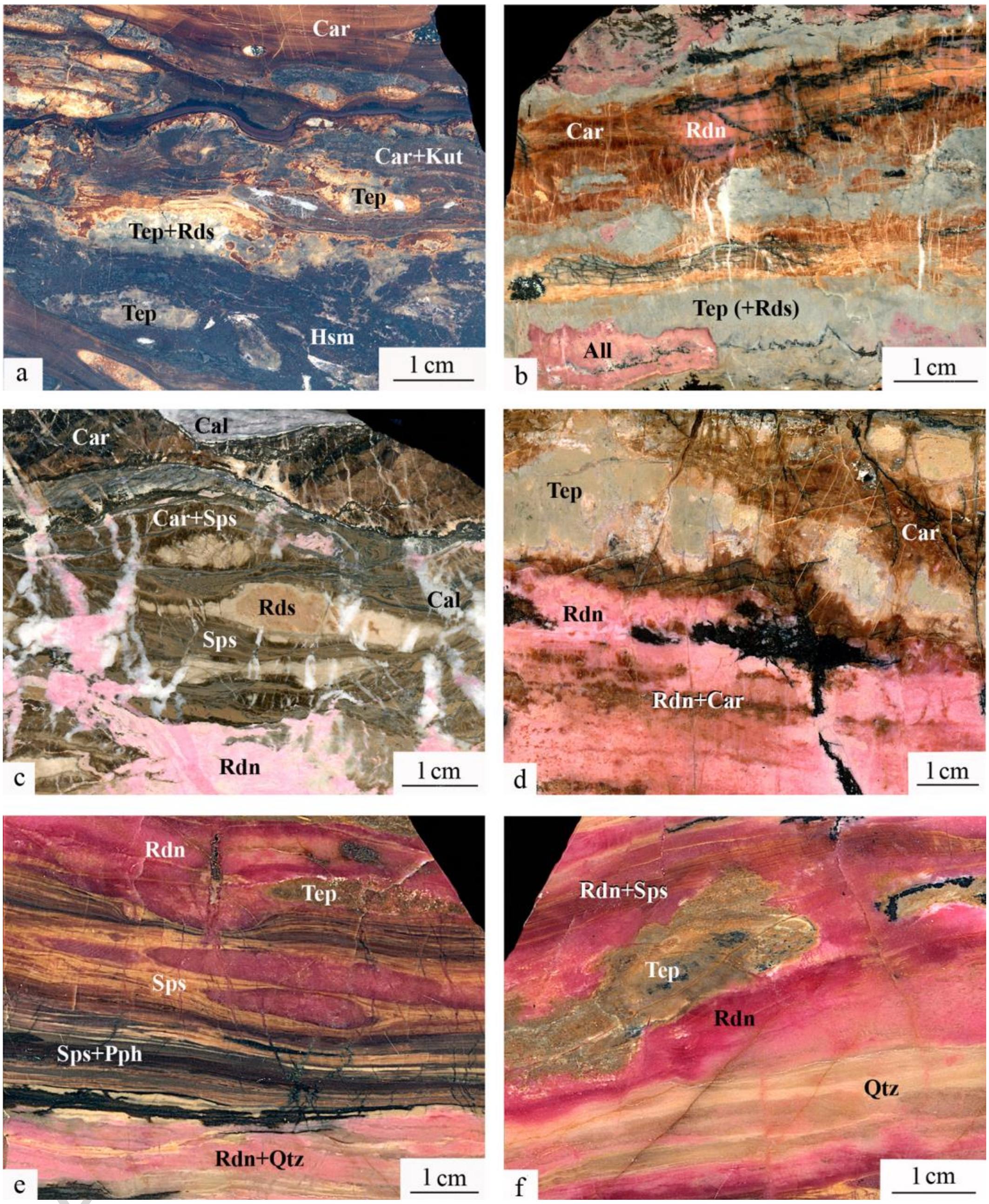
Car
Car+Kut
Tep
Tep+Rds
Tep
Hsm
a
1 cm
Car
Rdn
Tep (+Rds)
All
b
1 cm
Car
Cal
Car+Sps
Rds
Cal
Sps
Rdn
c
1 cm
Tep
Car
Rdn
Rdn+Car
d
1 cm
Rdn
Tep
Sps
Sps+Pph
Rdn+Qtz
e
1 cm
Rdn+Sps
Tep
Rdn
Qtz
f
1 cm

Figure 2

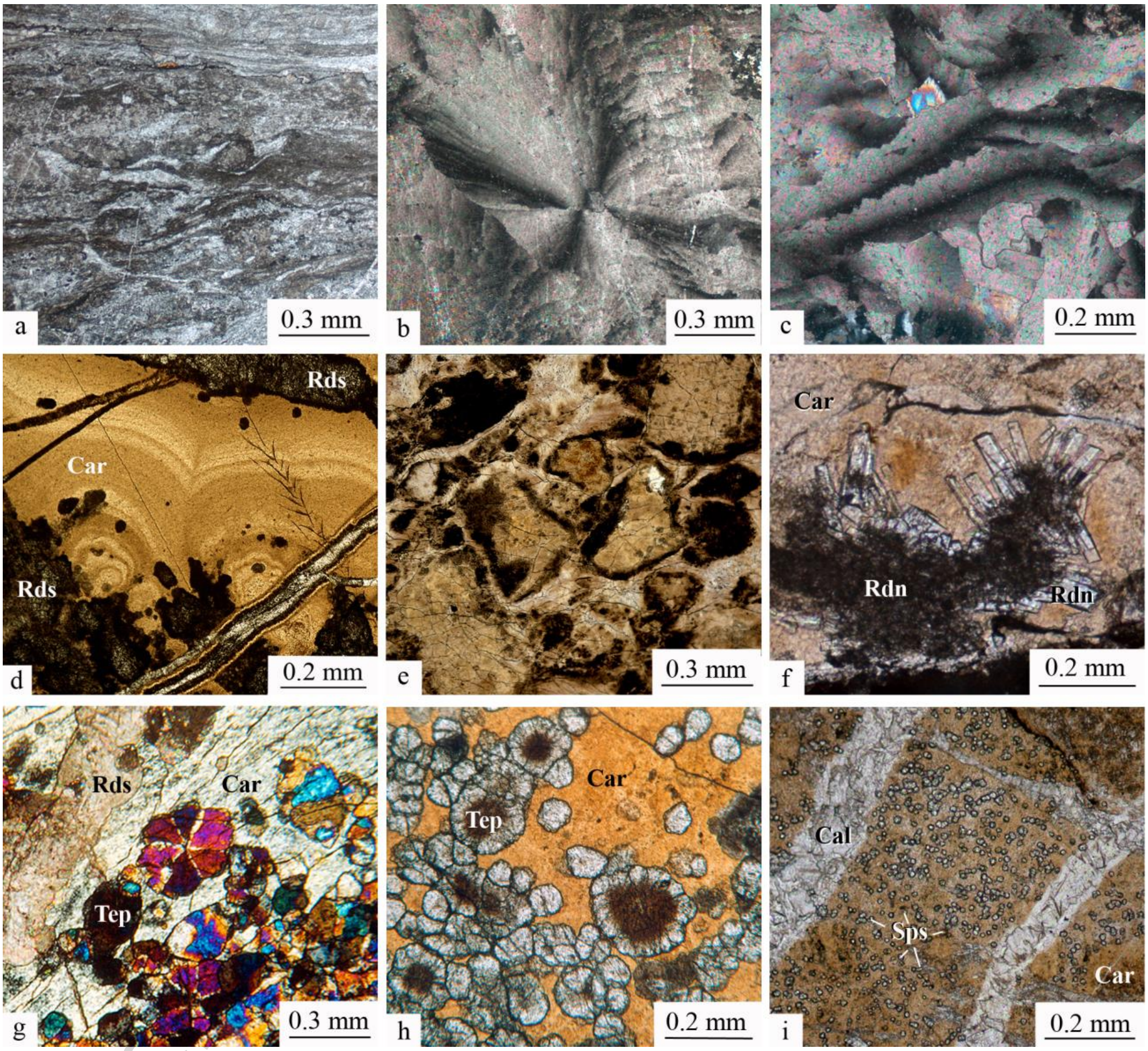
a
0.3 mm
b
0.3 mm
c
0.2 mm
Rds
Car
Rds
d
0.2 mm
e
0.3 mm
Car
Rdn
Rdn
f
0.2 mm
Rds
Car
Tep
g
0.3 mm
Car
Tep
h
0.2 mm
Cal
Sps
Car
i
0.2 mm

Figure 3

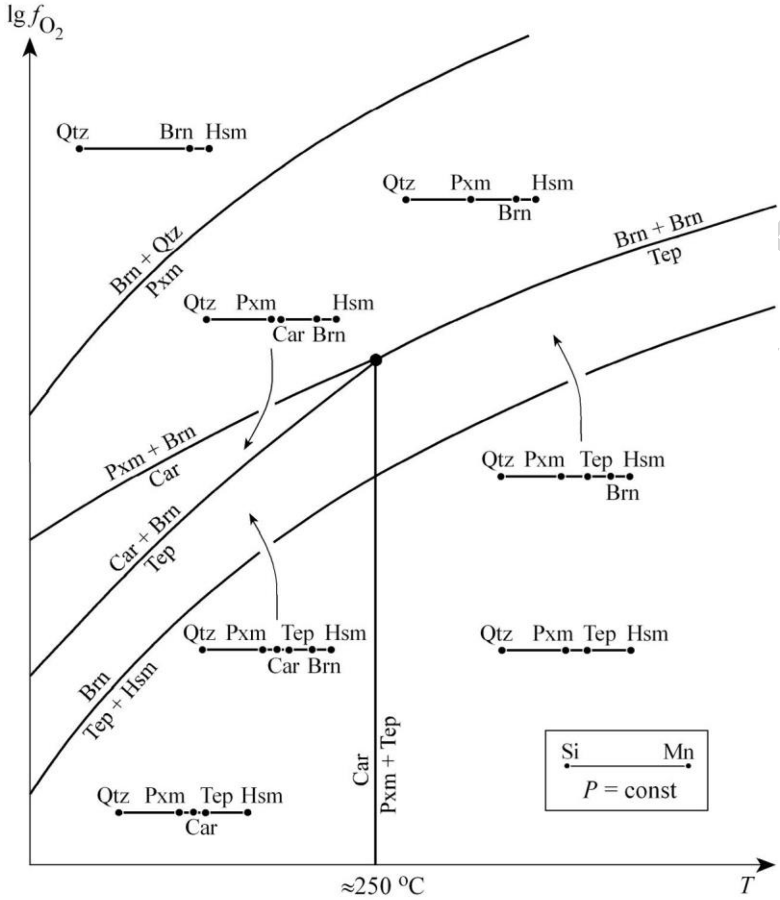
lg f_{O_2}
Qtz Brn Hsm
Brn + Qtz
Pxm
Qtz Pxm Hsm
Brn
Brn + Brn
Tep
Qtz Pxm Hsm
Car Brn
Pxm + Brn
Car
Car + Brn
Tep
Qtz Pxm Tep Hsm
Brn
Qtz Pxm Tep Hsm
Car Brn
Qtz Pxm Tep Hsm
Brn
Tep + Hsm
Car
Pxm + Tep
Si Mn
P = const
Qtz Pxm Tep Hsm
Car
≈250 °C
T

Figure 4

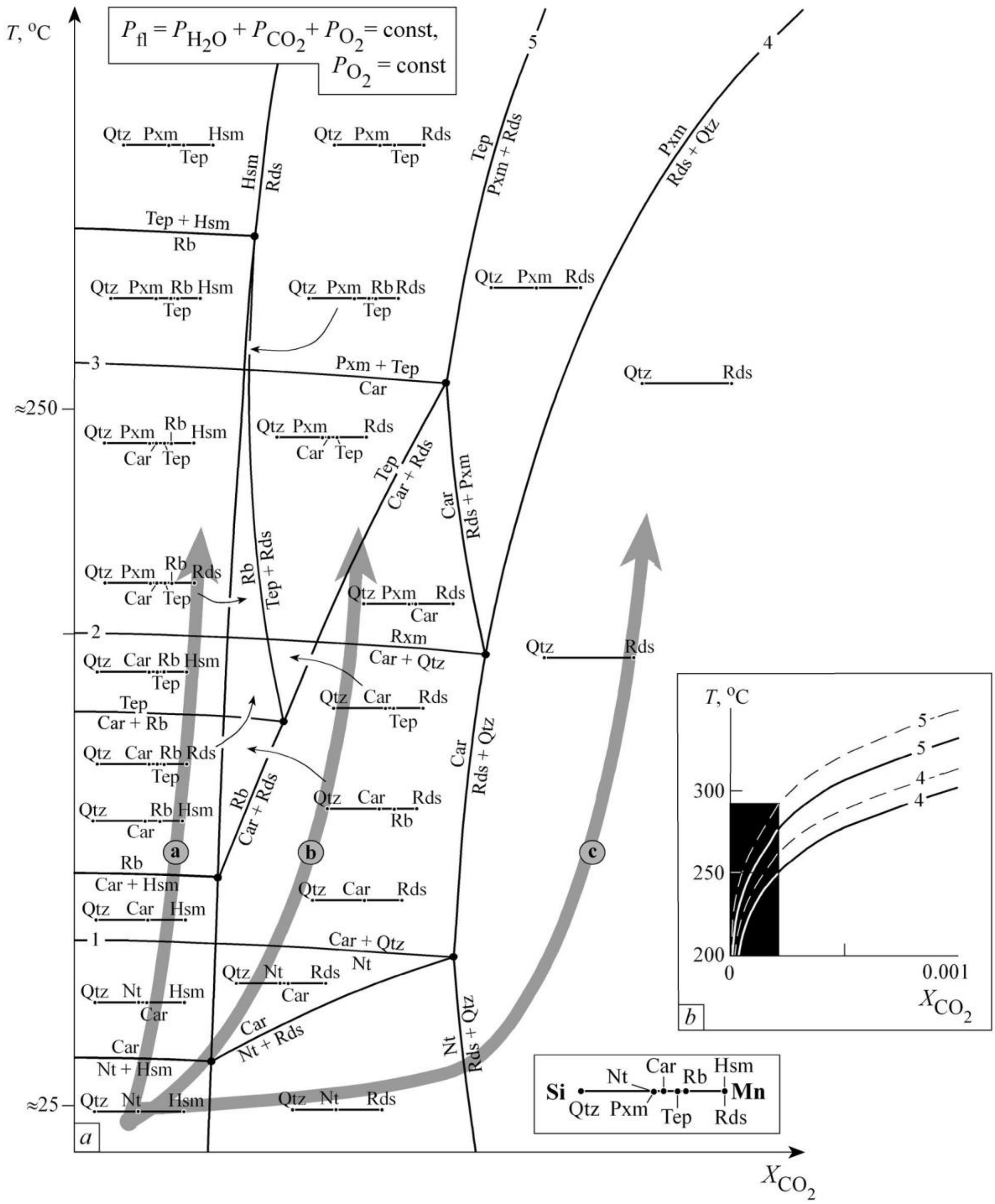
$P_{fl} = P_{H_2O} + P_{CO_2} + P_{O_2}$ = const,
P_{O_2} = const
T, °C
≈250
≈25
X_{CO_2}
Qtz Pxm Hsm Tep
Qtz Pxm Rds Tep
Tep + Hsm
Rb
Qtz Pxm Rb Hsm Tep
Qtz Pxm Rb Rds Tep
Qtz Pxm Rds
Pxm + Tep
Car
Qtz Rds
Qtz Pxm Rb Hsm Car Tep
Qtz Pxm Rds Car Tep
Qtz Pxm Rb Rds Car Tep
Qtz Pxm Rds Car
Rxm
Car + Qtz
Qtz Rds
Qtz Car Rb Hsm Tep
Tep
Car + Rb
Qtz Car Rds Tep
Qtz Car Rb Rds Tep
Qtz Rb Hsm Car
Qtz Car Rds Rb
Rb
Car + Hsm
Qtz Car Hsm
Qtz Car Rds
Car + Qtz
Nt
Qtz Nt Rds Car
Qtz Nt Hsm Car
Car
Nt + Hsm
Qtz Nt Hsm
Qtz Nt Rds
Hsm
Rds
Tep
Pxm + Rds
Pxm
Rds + Qtz
Rb
Tep + Rds
Car
Car + Rds
Car
Rds + Pxm
Car
Rds + Qtz
Nt
Rds + Qtz
Car
Nt + Rds
1
2
3
4
5
a
b
c
Si
Nt
Car
Rb
Hsm
Mn
Qtz
Pxm
Tep
Rds
T, °C
300
250
200
0
0.001
X_{CO_2}

Figure 5

Fig. 1. Location of main manganese deposits of the Urals, after (Mikhailov and Rogov, 1985; Mikhailov, 1993, 2001, 2011; Kontar et al., 1999; Puchkov, 2010; Brusnitsyn, 2013*a*; Starikova, 2014).

Manganese deposits: 1- Kheyakha, Sibirchatayakha (Late Devonian); 2- Lower Silova (Late Devonian); 3- Karsk (Late Devonian); 4- Silovayakha (Late Devonian); 5- Nadeiyakha-1 (Late Devonian); 6- Nadeiyakha-2 (Late Devonian); 7- Sob River basin (Late Devonian to Early Carboniferous); 8- Upper Tyshor (Proterozoic); 9- Parnok (Middle to Late Ordovican or Middle Devonian); 10- Verayu (Proterozoic); 11- Burmantovskoe (Late Cretaceous to Paleocene); 12- Pokunochnoe (Late Cretaceous to Paleocene); 13- Tyn'ynskoe (Late Cretaceous to Paleocene); 14- Berezovo (Late Cretaceous to Paleocene); 15- Yekaterino (Late Cretaceous to Paleocene); 16- Sapal (Late Silurian to Early Devonian); 17- Malosedelnikovo (Early Silurian); 18- Kurganovo (Early Silurian); 19- Borodulino (Early Silurian); 20- Klevakino (Late Devonian); 21- Ulutelyak (Permian); 22- Kozhaevo (Middle to Late Devonian); 23- Urazovo (Middle Devonian); 24- Bikkulovo (Middle to Late Devonian); 25- Kazgan-Tash (Middle to Late Devonian); 26- Kusimovo (Middle Devonian); 27- Kyzyl-Tash (Middle to Late Devonian); 28- South Fayzuly, souther part (Middle Devonian); 29- South Fayzuly, norther part (Middle Devonian); 30- Middle Fayzuly (Middle Devonian); 31- North Fayzuly (Middle Devonian); 32- Bakhtino (Devonian); 33- Kipchara (Early Carboniferous); 34- Akkerman (Early Carboniferous); 35- Shuuldak (Middle Devonian); 36- Shigrysh (Early Carboniferous); 37- Zilair (Middle Devonian); 38- Guberlya (Middle to Late Ordovican); 39- Kharkovo (Middle to Late Ordovican).

Fig. 2. Oxide–carbonate–silicate manganese rocks. (a–d) Caryopilite-bearing rocks of prehnite–pumpelliyte facies: (a) lens–banded caryopilite–carbonate–tephroite rock with hausmannite; (b) lens–banded rhodonite–caryopilite–tephroite rock with alleghanite lenses and stylolite boundary emphasized by black carbonaceous material in the bottom; (c) lens–layered rhodochrosite–spessartine–caryopilite rock with calcite and rhodonite veins; (d) banded caryopilite–tephroite–rhodonite rock (it is evident that rhodonite and tephroite are divided by a caryopilite layer; compare with fig. 2e); (e, f) caryopilite-free rocks of green schist facies: (e) banded quartz–spessartine–rhodonite rock; (f) lens–bedded quartz–rhodonite–tephroite rock with associated rhodonite and tephroite (compare Fig. 2d and 2f, see reaction 3 in Fig. 5). Qtz- quartz; Hsm- hausmannite; Pph- pyrophanite; Tep- tephroite; All- alleghanite; Sps- spessartine; Rdn- rhodonite; Car- caryopilite; Rds- rhodochrosite; Cal- calcite; Kut- kutnahorite. Deposits: (a) Kyzyl-Tash, (b–d) Parnok, (e, f) Malosedelnikovo. Polished samples.

Fig. 3. Structure of carbonate and oxide–carbonate–silicate manganese rocks: (a) pelitomorphic carbonate rock with lenticular-banded structure: variation of color are caused by different contents of rhodochrosite, manganese silicates and finely dispersed organic matter; (b) carbonate spherulite made up of radial intergrowths of finely acicular rhodochrosite; (c) granular structure formed by split rhodochrosire crystals; (d) concentrically-zonal caryopilite aggregate intergrown with early rhodochrosite and rhodochrosite veinlet of second generation; (e) pseudobrecciated caryopilite aggregate with numerous syneresis fractures caused by dehydration of watered Mn–Si substrate; (f) two generations of rhodonite in caryopilite aggregate: early clotted rhodonite is overgrown by late tabular rhodonite crystals; (e, f) radial intergrowths (twins) of tephroite in caryopilite matrix; (i) spessartine grains in caryopilite aggregate with calcite veinlets. Tep- tephroite; Sps- spessartine; Rdn- rhodonite; Car- caryopilite; Rds- rhodochrosite; Cal- calcite. Deposits: (a, b, c, i) Parnok, (d, g, h) South Fayzuly (southern part), (e) Bikkulovo. Transmitted light. Photos (a, d, e, f, h, i), ||nicols, (b, c, g) × nicols.

Fig. 4. $T-lgf_{O2}$ diagram for Mn–Si system after Brusnitsyn (2013*a*). Brn- braunite; Pxm- pyroxmangite; Tep- tephroite; Car- caryopilite; Hsm- hausmannite; Qtz- quartz.

Fig. 5. $T-X_{CO2}$ diagram for Mn–Si system after Brusnitsyn (2006, 2013*a*): (a) qualitative diagram for the complete system; (b) quantitative calculation of position of lines of reactions 4 and 5 (solid and dotted lines correspond to pressure of 2 and 3 kbar, respectively). Black rectangle, an area of diagram in Fig. 6a. Nt- neotocite; Car- caryopilite; Pxm- pyroxmangite (rhodonite); Tep- tephroite; Rb- ribbeite (alleghanite); Rds- rhodochrosite; Hsm- hausmannite; Qtz- quartz. Arrows **a**, **b** and **c** show the direction of processes of mineral formation in weakly metamorphosed sediments with low (a), moderate (b), and high (c) contents of organic matter.

Table 1

Characteristics of manganese deposits of the Urals

Notes. * Numbers of deposits correspond to those in Fig. 1. Facies of metamorphism: PP, prehnite-pumpellyite; GS, green schist. Mineral types of manganese rocks: «reduced» carbonate (I) and oxide–carbonate–silicate (II) and «oxidized» oxide–silicate (III) (see subdivision for groups a–j in text). 1 - only minerals from manganese ores are shown for the Parnok deposit.

Table 2

Minerals of manganese ores of the Urals

Notes. Modified after (Shishkin and Gerasimov, 1995; Brusnitsyn, 1998, 2000, 2010, 2013a, 2015; Brusnitsyn et al., 2000, 2009; Gerasimov et al., 1999; Starikova and Zavileisky, 2010; Starikova, 2011, 2014; Brusnitsyn and Zhukov, 2005, 2012). * Numbers of deposits correspond to those in Fig. 1. 1, only minerals of manganese ores are shown.

Table 3

Carbon isotopic composition of carbonates from manganese rocks of the Urals

Notes. * Numbers of deposits correspond to those in Fig. 1. Modified after Kuleshov and Brusnitsyn (2005); Brusnitsyn (2013a); Brusnitsyn et al. (2014); Kuleshov et al. (2014). 1: an area of braunite–rhodonite rocks with Mn-calcite.

Table 1
Characteristics of manganese deposits of the Urals

№*	Deposit	Host rocks	Age	Meta-morphism	Minerals of manganese rocks	
					Type	Major minerals
Hosted in sedimentary rocks of passive paleocontinental margin (deposit of the Pai Khoi and Polar Urals)						
1	Kheayakha, Sibirchatayakha	Jasper, organic clayey–calcareous–siliceous and siliceous shale (black shale)	Late Devonian	PP–GS	I*c*	Quartz, kutnahorite
2	Lower Silova	Jasper, organic clayey–calcareous–siliceous and siliceous shale (black shale)	Late Devonian	PP–GS	I*c*	Quartz, kutnahorite
3	Karsk	Jasper, organic siliceous shale (black shale)	Late Devonian	PP–GS	I*a*	Quartz, rhodochrosite
4	Silovayakha	Clayey–siliceous shale	Late Devonian	PP–GS	II*e*	Quartz, rhodonite, pyroxmangite, friedelite, rhodochrosite
5	Nadeiyakha-1	Clayey–calcareous–siliceous shale	Late Devonian	PP–GS	II*e*	Quartz, tephroite, sonolite, pyroxmangite, friedelite, rhodochrosite, kutnahorite
6	Nadeiyakha-2	Jasper	Late Devonian	PP–GS	II*g*	Quartz, hematite, rhodonite, orthoclase
7	Sob River basin	Organic siliceous and clayey–siliceous shale (black shale)	Late Devonian to Early Carboniferous	PP–GS	I*b*	Quartz, rhodochrosite, siderite, shamosite
					II*e*	Quartz, spessartine, pyroxmangite, friedelite, rhodochrosite
9	Parnok[1]	Organic clayey–siliceous–calcareous shale (black shale) and limestouns	Middle to Late Ordovican or Middle Devonian	PP	I*a*	Rhodochrosite
					II*d*	Hausmannite, pyrochroite, tephroite, calcite, rhodochrosite
					II*e*	Tephroite, sonolite, alleghanite, ribbeite, spessartine, rhodonite, caryopilite, friedelite, calcite, rhodochrosite
Hosted in volcanosedimentary rocks of active paleocontinental margin (deposit of the Central and South Urals)						
17	Malosedelnikovo	Organic clayey–siliceous shale (black shale), quartzite	Early Silurian	GS	II*f*	Quartz, tephroite, sonolite, alleghanite, spessartine, rhodonite, pyroxmangite, rhodochrosite
18	Kurganovo	Organic clayey–siliceous	Early Silurian	GS	II*f*	Quartz, tephroite, spessartine, rhodonite, rhodochrosite

№*	Deposit	Host rocks	Age	Meta-morphism	Type	Major minerals
		shale (black shale), quartzite				
19	Borodulino	Organic clayey–siliceous shale (black shale), quartzite	Early Silurian	GS	II*f*	Quartz, tephroite, sonolite, alleghanite, rhodonite, spessartine, calcite, rhodochrosite
22	Kozhaevo	Jasperite, jasper	Middle to Late Devonian	PP	II*d*	Hausmannite, tephroite, caryopilite, rhodochrosite
					II*e*	Hematite, tephroite, spessartine, andradite, grossular, rhodonite, albite, rhodochrosite
23	Urazovo	Jasperite, jasper, volcaniclastic rocks	Middle Devonian	PP	II*g*	Andradite, epidote, rhodonite, caryopilite, calcite
					II*h*	Quartz, epidote, piemontite

Table 1 (continued)

№*	Deposit	Host rocks	Age	Meta-morphism	Minerals of manganese rocks	
					Type	Major minerals
24	Bikokulovo	Jasperite, jasper, volcaniclastic rocks	Middle to Late Devonian	PP	II*d*	Hausmannite, tephroite, caryopilite, rhodochrosite
					II*e*	Quartz, hematite, tephroite, andradite, epidote, piemontite, pumpellyite-Mg, rhodonite, caryopilite, parsettensite, calcite, rhodochrosite
					II*h*	Quartz, epidote, pumpellyite-Mg, pumpellyite-Mn, parsettensite, calcite
25	Kazgan-Tash	Jasperite, jasper	Middle to Late Devonian	PP	II*e*	Quartz, hematite, tephroite, andradite, grossular, epidote, rhodonite, caryopilite, calcite
26	Kusimovo	Jasper	Middle Devonian	PP	III*i*	Quartz, hematite, braunite
					III*j*	Braunite, piemontite, rhodonite, caryopilite, parsettensite, calcite
27	Kyzyl-Tash	Jasperite, jasper	Middle to Late Devonian	PP	II*d*	Hausmannite, tephroite, caryopilite, rhodochrosite, kutnahorite
					II*e*	Quartz, hematite, tephroite, spessartine, andradite, grossular, epidote, rhodonite, caryopilite, calcite, rhodochrosite
28	South Fayzuly (southern part)	Jasperite, jasper, siliceous shale	Middle Devonian	PP	II*d*	Hausmannite, tephroite, alleghanite, ribbeite, caryopilite, rhodochrosite
					II*e*	Quartz, tephroite, alleghanite, ribbeite, spessartine, pyroxmangite, caryopilite, rhodochrosite
29	South Fayzuly (northern part)	Jasper	Middle Devonian	PP	III*i*	Quartz, hematite, braunite
30	Middle Fayzuly	Jasperite, jasper	Middle Devonian	PP	II*g*	Quartz, hematite, andradite, rhodonite
31	North Fayzuly	Jasper	Middle Devonian	PP	III*i*	Quartz, hematite, braunite

Notes. * Numbers of deposits correspond to those in Fig. 1. Facies of metamorphism: PP, prehnite-pumpellyite; GS, green schist. Mineral types of manganese rocks: «reduced» carbonate (I) and oxide–carbonate–silicate (II) and «oxidized» oxide–silicate (III) (see subdivision for groups a–j in text). [1] - only minerals from manganese ores are shown for the Parnok deposit.

Table 2

Minerals of manganese ores of the Urals

Minerals	Formulae	Deposit *																			
		Hosted in sedimentary rocks							Hosted in volcanosedimentary rocks												
		1, 2	3	4	5	6	7	9[1]	17	18	19	22	23	24	25	26	27	28	29	30	31
Silver	Ag	+										+									
Copper	Cu													+							
Acanthite	Ag_2S	+	+					+													
Alabandine	MnS			+	+			+	+	+	+							+			
Galena	PbS	+			+	+		+										+			
Clausthalite	PbSe	+																			
Altaite	PbTe					+															
Sphalerite	ZnS	+			+			+										+			
Pyrrhotite	FeS							+			+										
Millerite	NiS							+													
Nickeline	NiAs							+		+											
Molybdenite	MoS_2																	+			
Chalcopyrite	$CuFeS_2$	+						+				+			+			+			
Pentlandite	$Fe_5Ni_4S_8$																	+			
Cobaltpentlandite	Co_9S_8							+													
Siegenite	$CoNi_2S_4$	+																			
Pyrite	FeS_2	+	+	+	+		+	+	+	+	+	+			+			+			+
Arsenopyrite	FeAsS																	+			
Gersdorffite	NiAsS							+										+			
Cobaltite	CoAsS	+			+			+													
Ullmannite	NiSbS								+												
Aleksite	$PbBi_2Te_2S_2$							+													
Aikinite	$PbCuBiS_3$	+																			

Quartz	SiO_2	+	+	+	+	+	+	+	+	+	+	+	+	+	+	+	+	+	+	+	+

Table 2 (continued)

Minerals	Formulae	Deposit *																			
		Hosted in sedimentary rocks							Hosted in volcanosedimentary rocks												
		1, 2	3	4	5	6	7	9[1]	17	18	19	22	23	24	25	26	27	28	29	30	31
Rutile	TiO_2							+	+												
Hematite	Fe_2O_3					+	+					+	+	+	+	+	+	+	+	+	+
Ilmenite	$FeTiO_3$	+					+														
Pyrophanite	$MnTiO_3$	+				+	+	+	+	+	+	+	+				+	+			
Hausmannite	$Mn^{2+}Mn^{3+}{}_2O_4$							+				+		+			+	+			
Jacobsite	$FeMn^{3+}{}_2O_4$							+				+		+	+						
Magnetite	$Fe^{2+}Fe^{3+}{}_2O_4$		+				+	+						+	+		+				
Galaxite	$MnAl_2O_4$								+	+											
Hubnerite	$MnWO_4$										+										
Hollandite	$Ba(Mn^{3+},Mn^{4+})_8O_{16}$															+					
Pyrochroite	$Mn(OH)_2$							+													
Braunite-I	$MnMn_6(SiO_4)O_8$															+			+		+
Tephroite	Mn_2SiO_4			+	+		+	+	+	+	+	+		+	+		+	+			
Sonolite	$Mn_9(SiO_4)_4(OH)_2$			+	+			+	+	+											
Alleghanite	$Mn_5(SiO_4)_2(OH)_2$			+				+	+	+								+			
Ribbeite	$Mn_5(SiO_4)_2(OH)_2$							+				+						+			
Zircon	$ZrSiO_4$	+					+	+													
Spessartine	$Mn_3Al_2(SiO_4)_3$			+			+	+	+	+	+	+					+	+			
Andradite	$(Ca,Mn)_3Fe_2(SiO_4)_3$											+	+	+	+		+			+	+
Grossular	$(Ca,Mn)_3Al_2(SiO_4)_3$											+			+		+				
Titanite	$CaTi(SiO_4)O$							+				+	+	+							
Gageite	$Mn_{21}(Si_4O_{12})_2O_3(OH)_{20}$							+													
Zoisite	$Ca_2Al_3(SiO_4)(Si_2O_7)O(OH)$							+													
Epidote	$(Ca,Mn)_2FeAl_2(SiO_4)(Si_2O_7)O(OH)$												+	+	+		+				
Piemontite	$Ca_2MnFe_2(SiO_4)(Si_2O_7)O(OH)$											+	+	+		+	+	+			
Allanite-Ce	$(CaCe)(Fe,Mn)Al_2(SiO_4)(Si_2O_7)O(OH)$					+		+													

Table 2 (continued)

Minerals	Formulae	Deposit *																			
		Hosted in sedimentary rocks							Hosted in volcanosedimentary rocks												
		1, 2	3	4	5	6	7	9[1]	17	18	19	22	23	24	25	26	27	28	29	30	31
Pumpellyite-Mg	$(Ca,Mn)_2MgAl_2(SiO_4)(Si_2O_7)(OH)_2 \cdot H_2O$													+							
Pumpellyite -Fe	$(Ca,Mn)_2FeAl_2(SiO_4)(Si_2O_7)(OH)_2 \cdot H_2O$													+							
Pumpellyite -Mn	$Ca_2MnAl_2(SiO_4)(Si_2O_7)(OH)_2 \cdot H_2O$													+							
Ilvaite	$CaFe^{2+}{}_2Fe^{3+}(Si_2O_7)O(OH)$													+							
Hejtmanite	$BaMn_2TiO(Si_2O_7)(OH)_2$									+											
Manganaxinite	$Ca_2MnAl_2(BSi_4O_{15})(OH)$			+				+				+	+				+				
Johannsenite	$CaMn(Si_2O_6)$													+							+
Aegirine	$(Na,Mn)(Fe,Mn)(Si_2O_6)$																				+
Aegirine-augite	$(Na,Ca,Mn)(Fe,Mg,Mn)(Si_2O_6)$											+							+		+
Rhodonite	$CaMn_4(Si_5O_{15})$			+		+		+	+	+	+	+	+	+	+	+	+	+	+	+	+
Pyroxmangite	$Mn_7(Si_7O_{21})$			+	+		+	+	+						+	+		+			
Manganbabingtonite	$Ca_2MnFe(Si_5O_{14})(OH)$												+				+				
Manganocummingtonite	$Mn_2Mg_5(Si_8O_{22})(OH)_2$								+		+										
Actinolite	$(Ca,Mn)_2Mg_5(Si_8O_{22})(OH)_2$							+		+		+	+								
Ferriwinchite	$(CaNa)_2(Mg,Mn)_4Fe(Si_8O_{22})(OH)_2$																		+		+
Greenalite	$Fe_5(Si_4O_{10})(OH)_6$							+													
Caryopilite	$Mn_5(Si_4O_{10})(OH)_6$							+				+	+	+	+	+	+	+		+	
Friedelite	$Mn_8(Si_6O_{15})(OH,Cl)_{10}$			+	+		+	+													
Manganpyrosmalite	$Mn_8(Si_6O_{15})(OH,Cl)_{10}$																	+			
Bementite	$Mn_7(Si_6O_{15})(OH)_8$							+	+			+									
Kellyite	$Mn_2Al(AlSiO_5)(OH)_4$							+	+	+		+									
Talc	$Mg_3(Si_4O_{10})(OH)_2$											+			+			+			
Muscovite	$KAl_2(Si_3AlO_{10})(OH)_2$		+				+	+									+				
Phlogopite	$KMg_3(AlSi_3O_{10})(OH)_2$					+				+								+			
Shirozulite	$KMn_3(AlSi_3O_{10})(OH)_2$													+	+	+					
Wonesite	$Na_{0.5}(Mg,Fe,Al)_3[(Si,Al)_4O_{10}](OH)_2$					+															

Table 2 (continued)

Minerals	Formulae	Deposit *																			
		Hosted in sedimentary rocks							Hosted in volcanosedimentary rocks												
		1, 2	3	4	5	6	7	9[1]	17	18	19	22	23	24	25	26	27	28	29	30	31
Pennantite	$Mn_5Al(AlSi_3O_{10})(OH)_8$							+				+									
Clinochlore	$(Mg,Mn)_5Al(AlSi_3O_{10}(OH)_8$	+			+		+	+				+		+				+			
Shamosite	$(Fe,Mn)_5Al(AlSi_3O_{10}(OH)_8$						+	+							+						+
Stilpnomelane	$K(Fe^{2+},Mg,Mn)_8(AlSi_{11}O_{28})(OH)_8 \cdot 2H_2O$	+		+			+	+													
Parsettensite	$KMn_7(AlSi_9O_{24})(OH)_6 \cdot nH_2O$					+		+				+	+	+	+	+	+	+			+
Bannisterite	$KMn_{10}(AlSi_{15}O_{38})(OH)_8 \cdot nH_2O$										+	+		+	+						
Coombsite	$KMn_{13}(AlSi_{17}O_{42})(OH)_{14}$			+								+									
Zussmanite	$K(Fe,Mn)_{13}(AlSi_{17}O_{42})(OH)_{14}$			+																	
Neotocite	$Mn(SiO_3) \cdot nH_2O$			+					+	+	+	+		+			+	+			
Orthoclase	$K(AlSi_3O_8)$	+	+			+															
Albite	$Na(AlSi_3O_8)$					+	+					+							+		+
Celsian	$Ba(Al_2Si_2O_8)$			+				+	+	+						+					
Harmotome	$Ba(Al_2Si_6O_{16}) \cdot 6H_2O$											+									
Edingtonite	$Ba(Al_2Si_3O_{10}) \cdot 4H_2O$											+									
Calcite	$CaCO_3$	+	+	+	+	+	+	+		+		+	+	+	+	+	+	+			+
Rhodochrosite	$MnCO_3$	+	+	+	+	+	+	+	+	+	+	+		+	+	+	+	+			+
Siderite	$(Fe,Mn)CO_3$		+		+		+	+													
Kutnahorite	$CaMn(CO_3)_2$	+			+		+	+	+			+			+		+	+			
Dolomite	$(Ca,Mn)Mg(CO_3)_2$	+	+		+																
Ankerite	$(Ca,Mn)Fe(CO_3)_2$				+																
Barytocalcite	$CaBa(CO_3)_2$									+											
Calkinsite-Ce	$Ce_2(CO_3)_3 \cdot 4H_2O$							+													
Barite	$BaSO_4$	+		+	+	+		+	+			+	+	+	+	+	+			+	+
Monazite-Ce	$Ce(PO_4)$	+	+				+	+	+												
Xenitime-Y	$Y(PO_4)$						+														
Apatite	$Ca_5(PO_4)_3(F,OH)$	+	+	+		+	+	+			+	+	+	+	+	+	+	+			
Johnbaumite	$Ca_5(AsO_4)_3(OH)$											+									

Table 2 (continued)

Minerals	Formulae	Deposit *																				
		Hosted in sedimentary rocks							Hosted in volcanosedimentary rocks													
		1, 2	3	4	5	6	7	9[1]	17	18	19	22	23	24	25	26	27	28	29	30	31
Svabite	$Ca_5(AsO_4)_3F$											+									
Arsenoclasite	$Mn_5(AsO_4)_2(OH)_4$											+									
Brandtite	$Ca_2Mn(AsO_4)_2 \cdot 2H_2O$											+									
Decloizite	$PbZn(VO_4)(OH)$	+																			
Scheelite	$Ca(WO_4)$									+											
Bismoclite	BiOCl	+																			
Sussexite	$Mn(BO_2)(OH)$			+																	

Notes. Modified after (Shishkin and Gerasimov, 1995; Brusnitsyn, 1998, 2000, 2010, 2013a, 2015; Brusnitsyn et al., 2000, 2009; Gerasimov et al., 1999; Starikova and Zavileisky, 2010; Starikova, 2011, 2014; Brusnitsyn and Zhukov, 2005, 2012). * Numbers of deposits correspond to those in Fig. 1. [1], only minerals of manganese ores are shown.

Table 3
Carbon isotopic composition of carbonates from manganese rocks of the Urals

№*	Deposits	$\delta\ ^{13}C_{carb}$, ‰ (PDB)
	Deposit of Pai Khoi and Polar Urals	
1	Kheyakha	−0.8 ... −0.1
1	Sibirchathayakha	−2.0 ... 1.3
2	Lower Silova	−6.6 ... −1.1
3	Karsk	−10.2 ... −9.3
4	Silovayakha	−5.2 ... −2.9
5	Nadeiyakha-1	−16.4 ... −10.4
7	Sob River basin	−30.4 ... −11.9
9	Parnok	−17.1 ... −8.9
	Deposit of the Central and South Urals	
17	Malosedelnikovo	−21.9 ... −8.6
24	Bikkulovo	−29.3 ... −13.7
26	Kusimovo[1]	−22.0 ... −17.3
27	Kyzyl-Tash	−28.1 ... −10.8
28	South Fayzuly (southern part)	−51.4 ... −20.4

Notes. * Numbers of deposits correspond to those in Fig. 1. Modified after Kuleshov and Brusnitsyn (2005); Brusnitsyn (2013*a*); Brusnitsyn et al. (2014); Kuleshov et al. (2014). [1]: an area of braunite–rhodonite rocks with Mn-calcite.

Conflict of interest
No

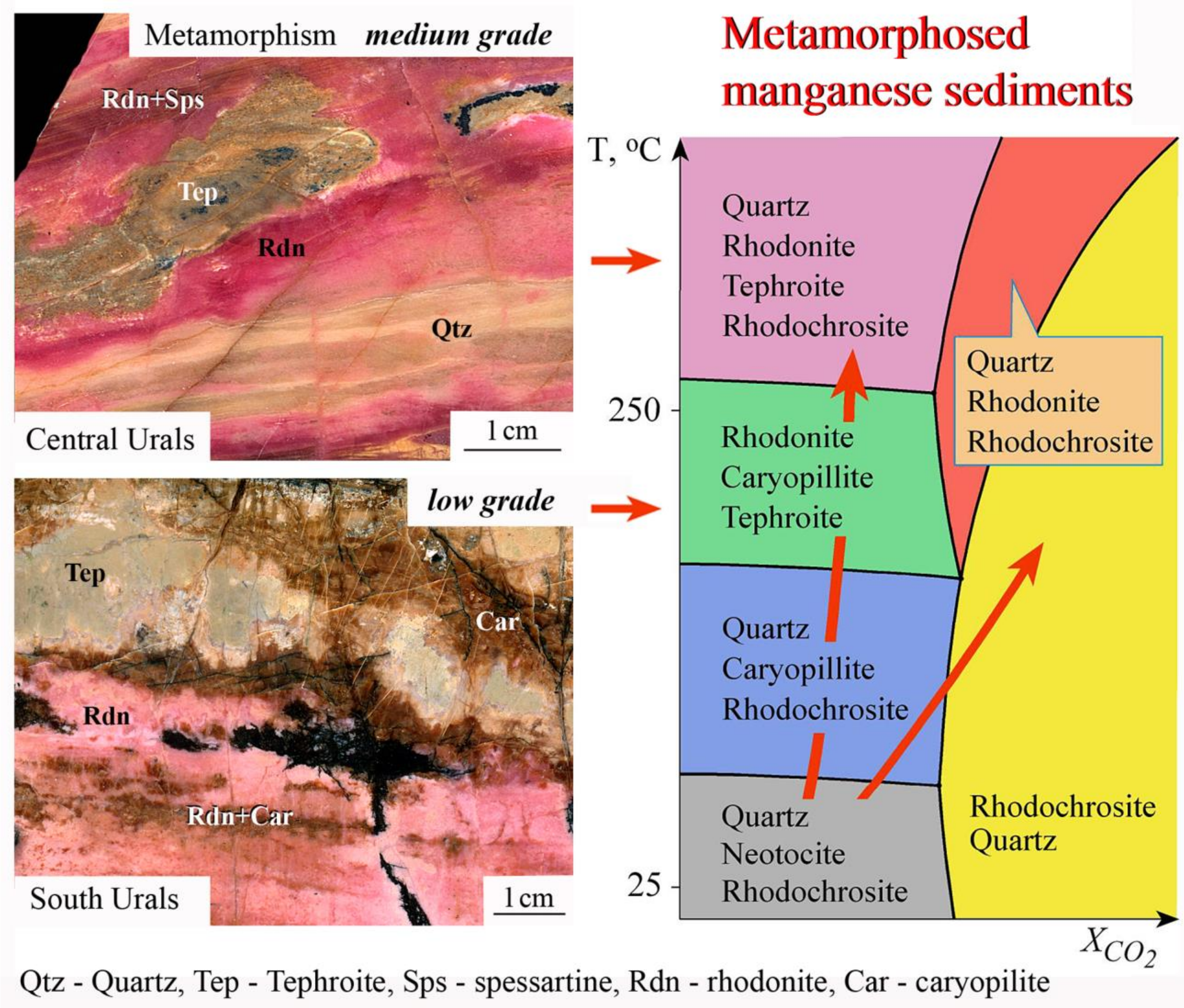

Graphical abstract

Highlights

- First study of the low grade metamorphosed manganese sediments from Urals.
- The rocks are subdivided to 3 types: I) carbonate, II) oxide-carbonate-silicate and III) oxide-silicate
- 104 minerals were identified in manganese rocks
- The rocks contain two different facies - low-temperature caryopilite and high-temperature caryopilite-free